Environmental Science: Atmospheres

ROYAL SOCIETY OF CHEMISTRY

CRITICAL REVIEW

View Article Online
View Journal | View Issue

Cite this: *Environ. Sci.: Atmos.*, 2024, **4**, 144

Electrical charging of snow and ice in polar regions and the potential impact on atmospheric chemistry

Kateryna Tkachenko †*[ab] and Hans-Werner Jacobi [b]

Charging of the ice–vapor interface is a well-studied topic in ice physics and atmospheric electrification. However, these effects were not yet considered to examine chemical processes in snow in polar regions because electric potentials at ice surfaces have so far been considered insufficient to initiate chemical reactions and processes. In this review, we analyze literature data to estimate levels of electrification in snow and other frozen objects that can be caused by different processes occurring at the Earth's surface. This analysis demonstrates that threshold values of electric field strength can be exceeded for the appearance of corona discharges and even for the formation of Rayleigh jets due to combined effects of different meteorological and physical processes. The accumulation of electrical charges can lead to different chemical modifications such as electroosmotic phenomena or the accumulation of impurities from the atmosphere in growing ice crystals. Moreover, highly energetic states that occur and dissipate in microseconds as "hot spots" have the potential to initiate free radical processes and even the production of charged aerosols. The review also discusses in detail selected field observations to point out how processes driven by electrical charging may help to interpret these observations, which are at least partly inconsistent with our present understanding of snow and ice chemistry. Finally, some approaches are presented how these effects can be studied in field and laboratory experiments. A further development of this new field at the intersection of ice physics and snow chemistry seems very promising for a better understanding of relevant chemical processes related to the cryosphere.

Received 9th June 2023
Accepted 15th January 2024

DOI: 10.1039/d3ea00084b

rsc.li/esatmospheres

Environmental significance

The role of chemical reactions in snow and ice for the atmospheric composition in polar regions is now well established, but mostly focusing on photo chemical reactions. However, well-known physical and meteorological processes can also lead to high electrical charging of snow and ice. In this critical review we analyze the potential charges that can occur under natural conditions and the chemical transformations that these charges are capable to initiate. Taking into account such processes due to electrostatic forces help to explain many poorly understood phenomena, some of them having been discussed for decades. They also open the possibility of chemical transformations under meteorological conditions that are so far considered as unfavorable (*e.g.* during the polar night) or even enable completely new chemical mechanisms.

1. Introduction

Until the end of the last century the snow cover in polar regions was mainly viewed as a sink of atmospheric trace compounds. In 1999, Honrath *et al.*[1] demonstrated that sunlit polar snow can transform deposited species like nitrate into volatile compounds that are reemitted to the atmosphere. As a result, the levels of a number of reactive species above the snow cover are significantly higher than expected if only long-range transport into the polar regions is considered. The polar snow cover acts as a chemical reactor,[2] and chemical reactions in the snow not only affect the levels of different chemical substances in snow, but also the composition of the atmospheric boundary layer above the snow especially in polar regions. The snow/atmosphere distribution of many chemical compound cannot be described only by chemical equilibria and adsorption processes.[3] Photochemical reactions in snow appeared in the focus of polar researches related to ice cores,[4] atmospheric chemistry,[2] the oxidation potential in the boundary layer above the ice shields in Greenland and Antarctica,[5] and pollution[6] leading to a strong increase of the number of snow photochemistry studies since 2000.[2] However, while the vast majority of the studies considered only photochemical processes for chemical transformations, observed concentrations of several species were even higher than those predicted by photochemical models (*e.g.* (ref. 7 and 8)). Such discrepancies may be reconciled if further mechanisms also initiating chemical reactions in snow are considered.

[a]*Institute of Geological Science (IGS), National Academy of Science of Ukraine, 01054, Gonchara Str 55b, Kyiv, Ukraine. E-mail: tkachenko.katya@gmail.com*

[b]*Institute for Geosciences and Environmental Research (IGE), Université Grenoble Alpes/CNRS/Grenoble INP/INRAE/IRD, 38000 Grenoble, France*

† Previously used name: Ekaterina Yu. Tkachenko

Here, we analyze the possible role of electrical phenomena in triggering chemical reactions in snow. The Lenard effect, also known as balloelectricity, refers to the phenomenon of water droplets being charged through splashing and spraying. This effect has been known since the 19th century (*e.g.* (ref. 9–11)), yet its underlying mechanism remains under ongoing investigation.[12] Recently, it was shown by Lee *et al.*[13] and confirmed by Mehrgardi *et al.*[14] that sprayed water microdroplets are able to generate H_2O_2. Since electrostatic processes can modify the chemical composition of water droplets, it also seems plausible that this can happen in ice particles.

The charging of ice–vapor interfaces has been well studied in the field of atmospheric electricity mainly related to lightning and other atmospheric processes.[15–17] A more limited number of studies has also dealt with the electrification of snow during blowing snow events and snowstorms. First field measurements were made by Simpson in 1919,[18] whose observations were confirmed more than 20 years later.[19,20] The peak of interest in this topic was in the 1960ies[21–25] and included also measurements in Antarctica.[26] All these studies aimed to collect qualitative and sometimes quantitative results on the electrification of blowing snow. More recent observations are motivated in part by the effects that charging has on snow particle motion and saltation distances[27–29] and hence on avalanche risks[30] and the mass balance of ice sheets.[31]

Chemical consequences of atmospheric electricity processes are well known (*e.g.* (ref. 32)) and the conditions leading to the charging of ice particles in clouds can also be encountered at sea level. Nevertheless, electrical phenomena have so far rarely been discussed in the context of snow chemistry. In the 1990ies, Finnegan *et al.*[33] proposed that chemical reactions can occur in growing ice crystals. Ten years later, Shavlov *et al.*[34] observed an acceleration of the corrosion of metal caused by ice growth processes. Finally, Tkachenko and Kozachkov[35] – hypothesized that triboelectrification of snow during blizzards can lead to corona discharges with following free radical reactions, while Tkachenko[36,37] pointed out that sharp tips of grounded ice structures can accumulate significant electrical charges possibly leading to the emission of reactive bromine. Here, we review potential processes leading to ice surface charging depending on meteorological conditions like temperature and wind speed. Low temperatures play an important role in the stimulation of charging due to friction or other mechanisms and also because of the absence of a quasi-liquid layer on the ice surface at sufficiently low temperatures. We further estimate the strength of the electric fields that can be generated as well as the conditions required to enable corona discharges considering also that some of these charges dissipate relatively slowly, while some charges can dissipate very quickly like hot spots inside an ice medium. We also analyze for each process leading to the charging of snow and ice, which electric potential can be achieved and which changes in the chemical composition can potentially be initiated. Subsequently, we present a number of field studies to evaluate if electrical phenomena related to the discussed processes may help to explain the biases between expected and observed concentrations of some trace compounds and other poorly understood field data. Finally, we propose some approaches how to study these effects in field and laboratory experiments.

2. Factors generating a static electrification of snow and ice crystals

In this chapter, we describe briefly how macro- and microscale processes interact to cause enhanced electric fields in snow and ice crystals and we present the relationship between the electric field strength and relevant chemical processes. In the following sub-chapters, single processes occurring in snow generating electric fields are described and analyzed in detail.

2.1. Macro and micro scale electric fields and thresholds for the initiation of chemical processes

Electric fields in the atmosphere appear as a result of the redistribution of charges of opposite polarity on macro and micro scales. The Earth can be regarded as a spherical capacitor where the Earth surface constitutes a negatively charged inner sphere and the ionosphere a positively charged outer sphere. The atmosphere acts as an isolator within this capacitor with a non-uniform electric field strength. The maximum values are encountered close to the Earth surface with the field strength decreasing exponentially with altitude. The usual background electric field strength is about 130 V m^{-1} (ref. 32) and directed from the top to the Earth surface. While this macroscale electric field is always present, it is not sufficiently strong to stimulate chemical reactions. However, in the presence of charged clouds or due to geomagnetic phenomena like in auroral ovals, the direction of the electric field can flip and its value increase substantially. Even in these cases the background electric field is not sufficient for direct initiation of chemical reactions in snow and ice. Nevertheless, the enhanced background electric field has the potential to intensify the redistribution of charges causing a localized accumulation of charges at the microscale.[38] The combined effect of such microscale processes can lead to an increase in the macroscale electric field as observed during blizzards (see below).

When the wind blowing over consolidated snow is free of particles, changes in the electric field strength are small. With the addition of snow particles, however, the field strength increases significantly.[27] Dry snow is a loose material, which undergoes electrification when drifting snow particles are rubbed against each other and touch the underlying surface due to the mobilization caused by wind.[19–21,23,24] Such snow electrification achieves maximum values at low temperatures and high wind speeds. Reports of such events can already be found in personal accounts in the 1950ies of scientists spending the winter in Antarctica like described by Silin,[39] who stayed a full year at the Pionerskaya station in a zone influenced by katabatic winds: "when the wind increased, the snow carried particles of static electricity, and all the objects at the station were so electrified that if somebody brought a neon bulb to them, it started to glow, and sparks flew between the insulators. All this would

be amusing, but it damaged the accuracy of our instruments. And from time to time there were unique records in our logbook: 'strong electrification, no observations can be done' "[original text in Russian, translated by the authors].

Unfortunately, available literature data with quantitative measurements of electric parameters during blizzards and blowing snow events concern more moderate conditions. Nevertheless, while under fair-weather conditions it can be assumed that, the strength of the observed electric fields obtained during a blizzard increased by two orders of magnitude. For example, at a temperature of – 12 °C and wind speeds from 10 to 17 m s^{-1} a field strength of +30 kV m^{-1} was observed at 4 cm above the snow surface (Table 1). Table 1 summarizes available studies attempting to measure the electrification of snow during high wind speed conditions (a list of parameters, used symbols, and units is given in Table 3 in Annex 1). These atmospheric electric field values resulted from a combined influence of positively and negatively charged snow grains. Measurements of charge-to-mass ratios of snow grains were also conducted and each new study with improved equipment gave higher values than those reported previously.[26,40] The most recent data of snow charge-to-mass ratios were obtained by Schmidt *et al.*[27] during experiments performed in Wyoming resulting in values varying from +72 to −208 μC kg^{-1}. Schmidt *et al.*[27] concluded that earlier reported data with typical average charge-to-mass ratio on the order of −10 μC kg^{-1} were likely under-estimated. Since drifting particles with opposing charges coexist during saltation, the Faraday cage typically used to determine the charge-to-mass ratios during the experiments most likely registered only net values of opposing electrical charges.

In summary, macroscale electric fields during blizzards and storms appear as a result of the joint action of different microscale charging processes, but due to the positive feedback this macro fields stimulate and enhance microscale charging processes (see Chapter 2.9). The mechanisms of charge accumulation on ice particles are of interest for atmospheric physicists and, therefore, it has been studied extensively. It is still under debate, which mechanisms are the most important for thunderstorm electricity.[41–43] Here, we present a selection of processes that can be relevant for snow–air interactions since the resulting electric field strengths can achieve high values at the microscale. Depending on the field strength, different chemical processes are possible as demonstrated in Fig. 1.

If the electric field strength increases sufficiently it can reach the threshold of the oxidation potential of species present in the snow and ice. The value of the oxidation potential is different for each ion, but when it is achieved redox reactions become possible. If the electric field strength increases further it can overcome the threshold value of 10^6 V m^{-1} for corona discharges (this value is valid for a pressure of 1000 mbar,[44–46] it decreases with pressure and, thus, with altitude). The corona discharge can occur as a channel of energy dissipation and activates molecules in the zone of its influence with the subsequent formation of active species such as free radicals. When the electric field grows even further, it may overcome the Rayleigh limit leading to the direct emission of ions from the condensed to the gas phase.

Such highly energetic areas appear and disappear like pulses. Their lifetimes are different for various processes and also depend on the initial conditions. Shibkov *et al.*[47] studied the persistence of strong electric charges in ice measuring the electromagnetic emission (EME) frequency during the growth of ice from supercooled water. They observed EME frequencies on the order of $\sim 10^{-1}$ to10^2 Hz, which corresponds to 0.1 to 100 pulses per second, with a duration of the pulses from 10 ms to 10 s. They detected a further band of signals with EME frequencies between $\sim 10^3$ and 10^6 Hz corresponding to pulse durations from 1 μs to 1 ms. The authors attributed these observations to the development of cracks during growth, friction, *etc.*

2.2. Charging due to friction

The so-called 'asymmetric rubbing' mechanism consists in the separation of charges during friction as the result of temperature and concentration gradients.[15,25,48,49] Friction does not heat

Table 1 Values of electric field strengths *E* observed at different wind speeds

Temperature	Wind speed	*E*, maximum	Location	Reference
−5 to −6 °C	8 to 15 m s^{-1}	10 kV m^{-1}	Byrd station, Antarctica	26
−12.5 to −10.5 °C	10 to 17 m s^{-1}	+30 kV m^{-1}	Wyoming, USA	27
−22 to −24 °C	15 to 16 m s^{-1}	+26.2 kV m^{-1}	Iqaluit, Nunavut, Canada	28
−1.9 to −2.9 °C	>7 to 8 m s^{-1}	+10 kV m^{-1} −15 kV m^{-1}	Hermon, Israel	29

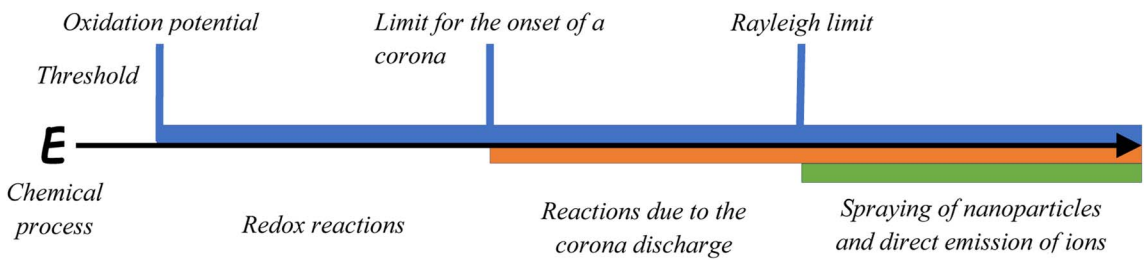

Fig. 1 Relationship between the electric field strength and different chemical processes and corresponding thresholds.

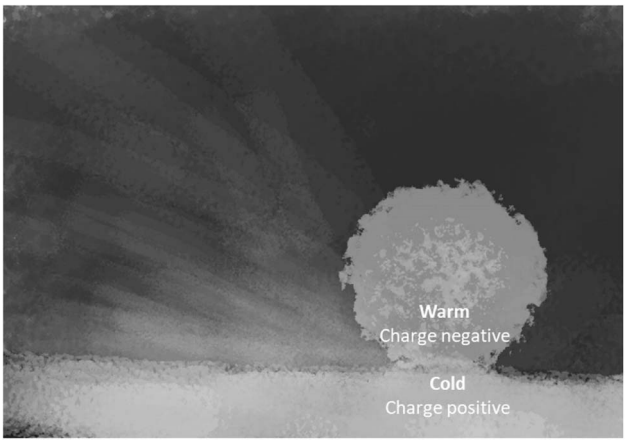

Fig. 2 Schematic representation of the effect of 'asymmetric rubbing' leading to electric charging of snow grains. Intensive friction creates higher temperature gradients and increases charge carrier concentration gradients because protons migrate faster toward cold regions.

ice surfaces homogeneously: the surface of the mobile ice is heated more strongly than the stationary ice surface (Fig. 2). The temperature gradient leads to an ion concentration gradient because protons (H^+) moves faster toward cold regions compared to hydroxide ions (OH^-).[48] Thus, the colder parts of the snow/ice particle obtain positive charges, while the warmer part becomes negatively charged (Fig. 2). This phenomenon is known as the thermoelectric effect.[50]

Petrenko and Colbeck,[41,51] who studied electromechanical properties of ice, found that friction electrification became stronger when the experimental temperature decreased. They measured the charging due to friction of a cylindrical ice sample made from very pure, deionized, and degassed water using 2.5 cm thick strips of polyethylene, aluminum, and stainless steel as sliders. The measurements were performed at temperatures T from −5 to −35 °C and friction velocities v varying from 0.5 to 8 m s^{-1}. When T was reduced from −10 °C to −35 °C, the observed that the charge density σ on the ice surface increased by an order of magnitude from 1.6×10^{-6} C m^{-2} to 10^{-5} C m^{-2}.

The electric field strength on the surface can be calculated according to eqn (1):

$$E = \sigma/\varepsilon_0 \quad (1)$$

with the permittivity of the vacuum $\varepsilon_0 = 8.85 \times 10^{-12}$ C V^{-1} m^{-1}.[52]

Thus, the electric field strength can be calculated as $E = 10^{-5}$ C $m^{-2}/8.85 \times 10^{-12}$ C V^{-1} $m^{-1} = 1.13 \times 10^6$ V m^{-1}, which is sufficient to overcome the threshold value for corona discharges (see Ch. 2.1). Moreover, while σ is proportional to v at $T = -10$ °C, it increases proportional to $v^{1.5}$, at $T = -14$ °C and to v^2 at $T = -25$ °C, so the decrease of temperature leads to a more and more rapid growth of the electric charge density.

2.3. Charging due to sublimation and ice crystal growth

It has been reported by many authors[16,53–55] that condensation growth and sublimation processes are accompanied by charging of the ice–vapor interface. The level of electrification is higher, the faster the ice crystal growth occurs.[16] When the growth stops, the charge diminishes. Various authors have interpreted this phenomenon differently. For example, the idea of the redistribution of impurity ions in the boundary layer of the growth zone was once popular.[55] Recently, many authors have agreed that the creation of charges at the interface is the result of different migration rates of the main charge carriers in ice during the rearrangement of the interface.[16,56,57] In ice, the

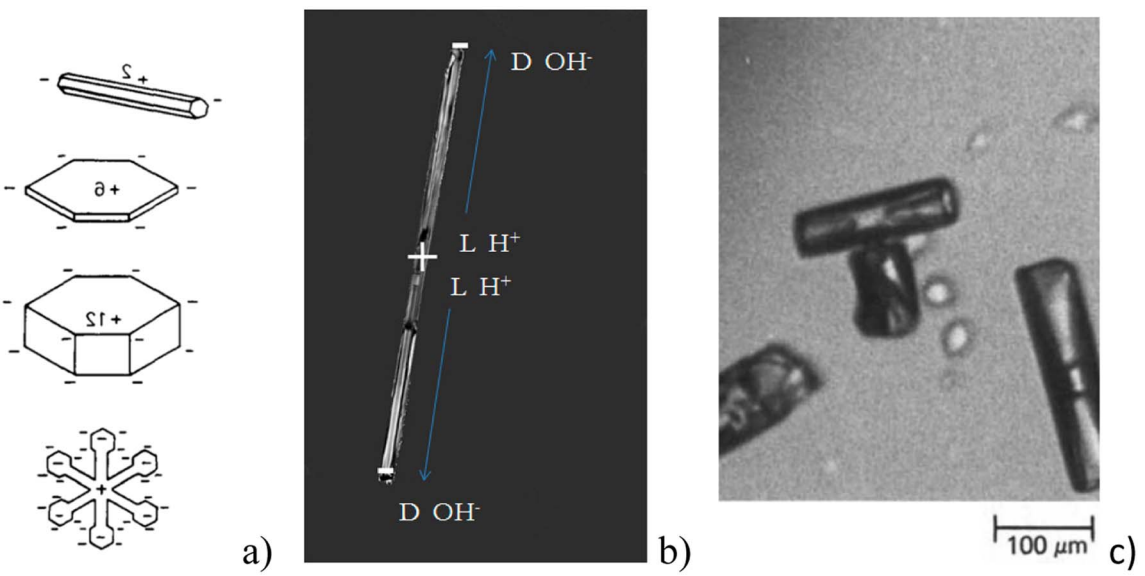

Fig. 3 (a) Charge distribution in growing ice crystals of various habits generating electric 'multipoles' (reproduced from ref. 61 with permission from Elsevier, copyright 1988); (b) distribution of charge during ice growth – H^+ and L^- defects are concentrated inside the crystal, OH- and D-defects on the tips; (c) T-shape ice crystal aggregates as a result of charging (reproduced from ref. 61 with permission from Elsevier, copyright 1988).

main charge carriers are Bjerrum defects,[58] H^+, and OH^- since ice is a proton semiconductor.[59,60] Bjerrum defects appear as a result of the proton mobility in the crystal lattice. Two protons between two oxygens are known as D(+) Bjerrum defect and a vacancy due to a missing proton corresponds to an L(−) Bjerrum defect. H^+, OH^-, and Bjerrum defects have different mobilities in ice. The charging of growing ice crystals has been observed in laboratory experiments[53–55] and was simulated in various studies (*e.g.* (ref. 16, 56 and 60)). The growth due to condensation is accompanied by the accumulation of D(+) defects and OH^- at the ice–air interface leading to an accumulation of L(−) defects and H^+ inside the crystal (Fig. 3). In the case of sublimation, however, the reverse mechanism is observed and H^+ and L(−) defects are accumulated at the interface. These are dynamic processes and the surface charges disappear quickly after stopping growth or sublimation. According to Nelson and Baker,[16] different ratios between concentrations of these basic charge carriers at the interface can explain the variety of measured experimental charge values.

According to Nelson and Baker[16] growth rates near 1 μm s^{-1} at −15 °C lead to an increase of the amount of Bjerrum defects and OH– on the surface by a factor of more than 10, resulting in a surface coverage c_{OH} of 8.4×10^{16} m^{-2}. Petrenko and Whitworth derived for the same conditions a value of 6×10^{15} m^{-2}.[60] The equivalent charge density σ is 10^{-4}–10^{-3} C m^{-2}. Using formula (1), the corresponding electric field at the surface corresponds to $E = 10^{-4}$ C $m^{-2}/8.85 \times 10^{-12}$ C V^{-1} $m^{-1} = 1.13 \times 10^7$ V m^{-1}, which is sufficient for overcoming the corona threshold value (see Ch. 2.1).

Recently, Mukherjee *et al.*[57] illustrated the electrification of the sharp tip of an ice crystal growing under the influence of a strong temperature gradient and, thus, humidity gradient. During their laboratory experiments they observed the detachment of ice fragments, which were attracted by a polar liquid film placed above the growing ice crystal. Mukherjee *et al.*[57] considered this system as a particle moving in the field of a capacitor and indirectly estimated the charge density of the ice crystal fragment from the measured time of flight and the size of the fragment. The estimated value of the surface charge density was 10^{-7} C m^{-2},[57] which is a few orders of magnitude smaller than the charge density calculated by Nelson and Baker.[16] Such differences may be due to the high temporal variability of the electric field indicating that Mukherjee *et al.*[57] possibly did not capture the maximum value during their experiments.

2.4. Charging due to cracking

According to Petrenko[42,62] a "frozen in" or "intrinsic" electrical field is present in both sea and freshwater ice due to the extrusion of impurity ions to the periphery of ice grains. If ice is split by a crack that grows rapidly in the direction perpendicular to this intrinsic electric field, surface charges of the opposite signs can be generated on the two surfaces of the crack with a maximum at the tip of the developing crack and a rapid decrease with distance and time.

Petrenko[42] estimated the maximum value of the electric field strength on the tip of a crack according to eqn (2)

$$E_{\perp}^{Cr} = \varepsilon_S \times E_{\perp} \quad (2)$$

where ε_S is the ice dielectric permittivity ($\approx$100) and $E_{\perp}$ is the component of the electric field perpendicular to crack surface.

If $E_{\perp}$ is about 100–1000 V m^{-1} according to the estimations by Petrenko,[62,63] the value of the electric field strength at the crack's tip is around $E_{\perp}^{Cr} = 10^4$–10^5 V m^{-1}.[42]

2.5. Charging due to cracking of ice during its growth/sublimation

Petrenko's algorithm[42] presented in Chapter 2.4 can be used for evaluation of $E_{\perp}^{Cr}$ resulting from the cracking of ice during its growth or sublimation. For the case of ice crystal growth, the intrinsic electric field $E_{\perp}$ appears as a result of redistribution of main charge carriers as it was discussed in Chapter 2.3. It is directed along the path of crystal growth (Fig. 3b) and to the opposite direction for the case of ice crystal sublimation. Situations of fast crystal growth or sublimation appear quite often under natural conditions. If these crystals are cracked as a result of their collision with each other or with other objects, cracks perpendicular to the direction of growth (or sublimation) can create "hot spots" with highly localized electric fields, like dots of flame in ice media (Fig. 4).

Using the charge density σ of the detached fragment observed by Mukherjee *et al.*[57] of 10^{-7} C m^{-2}, an intrinsic electric field strength can be estimated according to eqn (1) as $E_{\perp} = E = 1.13 \times 10^4$ V m^{-1}. The electric field strength at the tip of the crack developing rapidly perpendicular to this intrinsic electric field of a growing crystal corresponds to $E_{\perp}^{Cr} = 100 \times 1.13 \times 10^4$ V $m^{-1} = 1.13 \times 10^6$ V m^{-1} according to eqn (2), which is sufficient for overcoming the threshold of the corona discharge (see Ch. 2.1).

However, this high electric field in a "hot spot" dissipates within microseconds. Petrenko estimated a charge relaxation time τ_1 of $\sim 10^{-6}$ s for not-growing crystals of pure ice at −10 °C.[42]

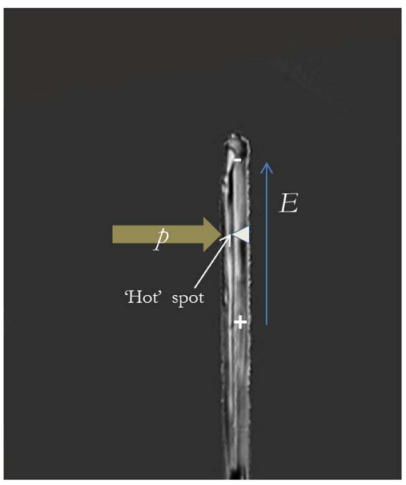

Fig. 4 Schematic presentation of the cracking of a growing column ice crystal (growth + cracking) under the influence of pressure (p). The blue arrow represents an electric field E. The 'Hot' spot is a point at the tip of a crack with a highly localized electric field $E_{\perp}^{Cr}$.

In natural ice, which is always doped by ions and impurities, this dissipation is even faster.[42] As a result, the impact of the electric field is limited to very short distances. As crack propagation velocity varies in the range from 100 to 1000 m s^{-1} (ref. 63 and 64) the highly charged space is likely limited to a radius of 0.1 to 1 mm.[42] It can be assumed that cracking during sublimation also creates similarly charged "hot spots", but their properties cannot be estimated due to a lack of initial data.

2.6. Charging due to the combined influence of cracking, growth, and friction

Charging of ice crystals under the combined influence of cracking, growing, and friction has been studied in laboratory experiments aimed to model atmospheric electricity processes.[17,65–67] Avila and Caranti[17] measured the charge transfer during the collision of ice particles with a target from a cylinder of ice growing by riming in a cold wind tunnel. The target was collided with ice spheres with a diameter of 100 μm at a speed of 5 m s^{-1} and in a temperature range from −10 to −24 °C. The transferred charge q ranged from −50 fC at higher to −80 fC at lower temperatures. A charge of ±50 fC is equivalent to an estimated surface charge density of 5×10^{-4} C m^{-2} corresponding to an electric field at the surface of 5.6×10^{7} V m^{-1} sufficient for exceeding the corona discharge limit. Keith and Saunders[68] detected light emission from corona discharges as a result of the collision of ice crystals and concluded that during contact of the colliding crystals large charge transfers occurred. Furthermore, they hypothesized that the net charge transfer remained small due to the breakdown of the corona. Overall, they observed approximately 10^4 photons per fC.

2.7. Charging of grounded objects

For each point in the Earth's atmosphere the electric field potential U can be calculated according to eqn (3).[69]

$$U = h \times E_o \quad (3)$$

where h is the height of the object's tip above the ground level (AGL) and E_o is the ambient electric field strength around the tip.

This electric field potential of a grounded conductor creates an electric field strength E at the tip. E depends on the radius r of the curvature of the conductor's tip and can be derived from eqn (4)

$$E = U/r, \quad (4)$$

The combination of eqn (3) and (4) results in eqn (5):

$$E = (h \times E_o)/r, \quad (5)$$

Thus, the electric field strength at the tip of a grounded conductor depends linearly on the ambient electric field E_o, the height above the ground level (or the conductor length in the case of a vertically oriented object) and it is inversely proportional to the radius of the tip of the conductor. Thus, a very sharp tip of grounded conductors leads to strong electric field gradients.

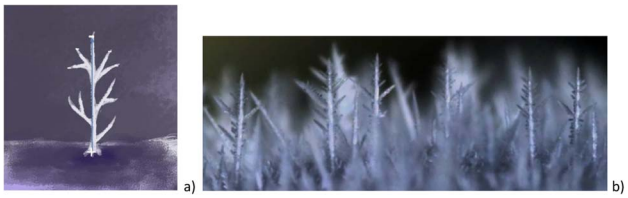

Fig. 5 (a) A schematic presentation of a frost flower as an example of an ice structure with a very sharp tip leading to a negative charge on the tip of the structure; (b) image of real frost flowers for comparison.

Since ice acts as a proton semiconductor,[59,60,63] it can conduct electric current. Tkachenko[36] considered frost flowers (Fig. 5) as grounded conductors and evaluated E at their tips. Frost flowers appear on freshly formed sea ice in the conditions of strong vertical temperature and humidity gradients. The temperature of thin sea ice is close to that of the sea water temperature in contact with the sea ice, which is normally about ~−2 °C. Lower temperatures can lead to a local oversaturation of the atmosphere in moisture and dendritic ice crystals form as long as these temperature and humidity gradients exist.[70,71] According to Gonda[72] the radius of a needle-like tip of a growing dendritic ice crystal is on the order of 7 to 15 μm. The tip remains sharp during the entire formation of the frost flower. Frost flower can reach heights of up to 10 cm above the sea ice surface.[71] The ambient electric field strength E_o of around 130 V m^{-1} (ref. 32) increases towards lower latitudes.[73] Therefore, we can estimate a lower limit of $E = 130$ V $m^{-1} \times 0.03$ m/10^{-5} m ≈ 4.2×10^5 V m^{-1} for the electric field strength E on the needle-like tip of a 3 cm high frost flower. When the radius is smaller, E increases. For example, a radius of 7 μm results in $E = 130$ V $m^{-1} \times 0.03$ m/(7×10^{-6}) m ≈ 5.6 10^5 V m^{-1}. Taller frost flowers also result in higher E: for instance, at the tip of a 10 cm high frost flower, E corresponds to approximately 1.85×10^6 V m^{-1}.

Galactic cosmic rays and also the interaction of the solar wind with the Earth's magnetosphere can significantly increase the ambient electric field strength E_o. It can increase up to an order of magnitude to reach values of about 1000 V m^{-1}.[74] In this case, the estimated electric field strength E can be as high as $E = 1000$ V $m^{-1} \times 0.03$ m/10^{-5} m ≈ 3 10^6 V m^{-1}.

When E is so high, even less high grounded objects, as surface hoar or frost flower with a height of 1 cm (ref. 75) can achieve field strengths of 10^6 V m^{-1}:

$$E = 1000 \text{ V m}^{-1} \times 0.01 \text{ m}/10^{-5} \text{ m} \approx 10^6 \text{ V m}^{-1}$$

Open water areas like polynyas or leads in the sea ice-covered regions can strongly impact atmospheric conditions, as the ambient electric field strength in their zone of influence increases. This happens because fog droplets trap "small ions" such as $NO_3^-(H_2O)_8$ and $H_3O^+(H_2O)_6$ that are responsible for atmospheric conductivity.[76] As a result, the conductivity in areas with "sea smoke" or sea fog consistently decreases. For

instance, Deshpande and Kamra[77] observed a change of total electric conductivity from ~2.3 to less than 0.7 S m during the period of sea fog. Since the electric field strength is inversely related to the conductivity, it increased by the same factor of approximately 3.5. This is an agreement with observations by Bering *et al.*,[76] who demonstrated that the decrease of conductivity in clouds can enhance the strength of the electric field by a factor of 3 to 30. Moreover, humidity gradients near the leads may stimulate the rapid growth of ice crystals with sharp tips. Under these conditions, surface hoar tips will be more charged due to higher ambient electric fields and smaller radii. For instance, if we use the same equation for 1 cm long hoar crystals[75] with a median radius of about 10 μm (ref. 72) and a 3.5 times stronger ambient electric field, the value of the electric strength on the tip of the surface hoar dendrite will be

$$E = 450\ \mathrm{V\ m^{-1}} \times 0.01\ \mathrm{m}/(10^{-5}\ \mathrm{m}) \approx 4.5\ 10^{5}\ \mathrm{V\ m^{-1}}.$$

An estimation for needle-like morphology with a minimum radius of 7.5 μm (ref. 72) and a 1.5 cm hoar height[75] gives $E = 450\ \mathrm{V\ m^{-1}} \times 0.015\ \mathrm{m}/(7.5\ 10^{-6}\ \mathrm{m}) \approx 9\ 10^{5}\ \mathrm{V\ m^{-1}}$.

This result is very close to the critical value of $10^{6}\ \mathrm{V\ m^{-1}}$ for the start of corona discharges. The examples given above show how even small changes in environmental conditions can result in achieving the threshold, after which corona discharges can appear. The morphology of the ice crystal, *i.e.* the crystal tip radius and length, depends on ambient temperature and humidity during the growth of the crystals.[78] If the ice tip radius has the size of about a few μm, even small changes in the average electric field strength due to diurnal or seasonal variations can turn corona discharges on or off. Significant changes of E_o by an order of magnitude during geomagnetic storms especially in the auroral zone in spring[74] or by two orders of magnitude during blizzards (Table 1) can make corona discharges also possible for crystals with not so sharp tips.

2.8. Fresh snow metamorphism – grounded system with growth/sublimation processes

Snow on the ground undergoes continuous re-organization until it reaches the most stable thermodynamic state. The metamorphism of snow has been intensively studied and the different stages and snow types have been described in detail (*e.g.* (ref. 79–81)). Since snow is close to its melting point, it can sublimate directly from the solid to the gas phase with following condensation at colder surfaces. The rates of the sublimation and condensation inside the snowpack strongly depend on the temperature as well as on the temperature gradient inside the snowpack. However, sublimation can occur even in an isothermal snowpack in order to reduce the surface area of the grains ultimately leading to rounded crystals. Maximum growth rates observed in laboratory experiments varied from 1.6 to $5 \times 10^{-7}\ \mathrm{kg\ m^{-2}\ s^{-1}}$ at temperature gradients from 16 to 50 $\mathrm{K\ m^{-1}}$ (*e.g.* (ref. 82–84)). As a result, 60% of the mass of freshly fallen snow can be redistributed within 12 hours[85,86] and after 2–3 days 100% of the freshly fallen snow may have undergone sublimation and condensation[83] depending on the strength of the temperature gradient.

Since the time of complete evaporation of an ice sphere (t) is proportional to the square of its radius,[87] small snow particles evaporate faster than large ones according to eqn (6):

$$t = \rho_c r^2/2D(e_n - e_\infty) \quad (6)$$

where t is the time of a complete evaporation of an ice sphere (s), r is the radius (m); ρ_c is the density of ice ($\mathrm{g\ m^{-3}}$); $(e_n - e_\infty)$ is the humidity deficit in the air, the difference between the saturation humidity e_∞, and the actual humidity e_n (g of water/$\mathrm{m^3}$ of air); and D is the diffusion coefficient of water vapour in the atmosphere ($\mathrm{m^2\ s^{-1}}$).

Sharp edges and branches of freshly fallen snowflakes evolve quicker and according to eqn (6) a particle with a radius of 0.1 mm disappears 100 times faster than a particle with a radius of 1 mm at the same humidity deficit.

When the sublimation of small crystals increases the moisture content in the pores of the snowpack up to the saturation value e_∞, new crystals start growing. The process progresses only in one direction – only large particles grow, *i.e.* small snow grains are reorganized into large ones making the snowpack over time coarse-grained.

According to eqn (6), the rate of sublimation (as well as growth) during metamorphism processes is highly variable in time with its maximum for freshly fallen snow. Available literature data about rate of snow growth due to metamorphism (from 1 to 3×10^{-3} $\mu\mathrm{m\ s^{-1}}$ according to ref. 88) can represent an average value.

Moreover, these initial snowflakes with small radiuses of their tips undergoing redistribution due to metamorphism can be considered as grounded conductors that concentrate the potential on their tips (Chapter 2.6). The increase of the radius leads to a decrease of this potential. Taking both of these considerations into account, freshly fallen snow can be understood as highly active electrodynamic system as described by Kazakov.[89]

2.9. Charging due to blizzards – combined influence of all factors

Blizzards create the most favorable conditions for friction and cracking of ice. The collision of cold and warm air masses under cold temperatures leads to snow formation. Therefore, ice crystals growth is most intensive at blizzard fronts. The conditions in the central area of a blizzard also stimulate sublimation processes because the turbulent mass exchange leads to the continuous removal of vapor-saturated air masses and their replacement by drier air.[87] The moisture deficit accelerates particle sublimation according to eqn (6) and high wind speeds intensify the friction and cracking. E_o increases during blizzards by two orders of magnitude up to 30 $\mathrm{kV\ m^{-1}}$ (ref. 27) (Chapter 2.1, Table 1).

Chapter 2.6 demonstrated how changes of ambient conditions can change E values at the sharp tips of grounded objects like frost flowers. Previous evaluations have shown how this value can be changed by conditions of geomagnetic storm or near polynya. If we use same algorithm for evaluation of electric field on the sharp tip of frost flower under the electric field produced by blizzard[26] it can be seen that E increases significantly:

$$E = 3 \times 10^4\ \mathrm{V\ m^{-1}} \times 3 \times 10^{-2}\ \mathrm{m}/(10^{-5}\ \mathrm{m}) \approx 10^8\ \mathrm{V\ m^{-1}}.$$

So, that overcoming of Rayleigh limit[90,91] becomes possible with "spraying" of submicro particles known as Rayleigh jets.[69,92] In other words, it leads to the production of small aerosol particles that will be discussed below (Ch. 3.6 and 4.4).

2.10. UV irradiation

Khusnatdinov and Petrenko,[93] who studied the electrolysis of ice, showed that the irradiation with UV in the range from 180 to 370 nm strongly increased the observed electric current (*i.e.* the number of charge carriers formed in the ice) contributing to an enhanced rate of the ice electrolysis (Fig. 6a). A larger number of free charge carriers increases the ability of the ice crystal to accumulate charges. As a result, the charging of ice by the different mechanisms described above such as friction, growth, *etc.* is potentially more effective under the influence of UV irradiation.

Fig. 6b presents a scheme how UV irradiation not only triggers photochemical reactions, but it can also increase the possibility of the enhancement of free radical processes due to a more efficient accumulation of electrical charges. How these two parallel processes can influence each other remains an open question.[94] For example, the radicals produced by both processes may interact with each other.

2.11. Summary

We demonstrate that friction, cracking, growth/sublimation as well as charging of grounded object described in the previous chapters appear as the most important processes for the electrical charging of snow and ice at the Earth's surface. These mechanisms have been considered since a long time in atmospheric electricity (*e.g.* (ref. 32)) and have been studied in ice physics laboratory experiments.[14–17,42,60,62] For each described process we examined literature data and estimated the potential electric field strengths that can be achieved. These values are summarized in Table 2. If only charge density values were available, they were used to recalculate electric field strengths using eqn (1). The combined influence of all mentioned mechanisms acting during storms and blizzards accompanied by high wind speeds and strong gradients in humidity can enhance the estimated values by a factor of hundred or more due to more effective friction, cracking, growth or sublimation of ice and snow.

In almost all cases the electric charges dissipate quickly. For instance, the charge at the tip of a newly-formed crack decreases within microseconds or even faster.[42] Growth/sublimation processes lead to more stable electrical fields, but as soon as the process stops, the charge also disappears.[16]

Since these highly charged states are quite transient and can dissipate in fraction of seconds, huge differences between laboratory (Table 2) and field values (Table 1) are possible. It is likely that the values of the charge-to-mass ratios of snow

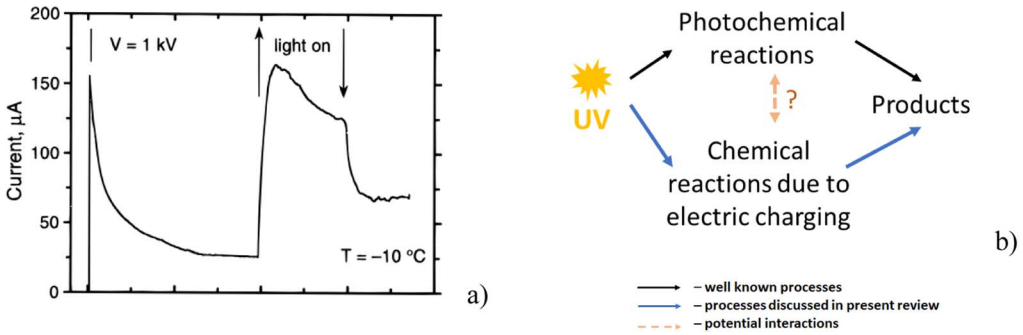

Fig. 6 (a) Increase of measured electric current due to the increase of the number of electric carriers caused by UV irradiation. The arrows indicate the time interval when the UV light was on (reproduced from ref. 93 with permission from American Chemical Society, copyright 1997); (b) schematic illustration of how UV irradiation initiates photochemical reactions with simultaneous influence on reactions stimulated by electric charging and possible interaction between these processes.

Table 2 Ranges of electric field strengths that can be achieved by different processes

Process	Range of field strengths [V m^{-1}]	Reference
Friction	Up to 1.13×10^6	42[b]
Growth/sublimation	1.13×10^4	57[b]
	1.13×10^7 (model)	16[b]
Cracking[a]	10^4 to 10^5	42[c]
(Cracking + growth)[a]	$\sim 1 \times 10^6$	Estimated value
(Cracking + growth + friction)[a]	$\sim 5 \times 10^7$	17[b,c]
Grounded objects	4×10^5 to up to 10^6	Estimated value
Friction + sublimation + cracking + grounded objects[a]	Up to 10^8	Estimated value

[a] Charge decreases within microseconds or even faster. [b] Charge density data. [c] Electric field strengths.

Table 3 List of parameters with used symbols and units

Parameter	Symbol	Unit
Temperature	T	°C
Charge density	σ	C m^{-2}
Velocity	v	m s^{-1}
Dielectric permittivity of ice	ε_S	
Component of the electric field perpendicular to the crack surface	$E_\perp$	V m^{-1}
Electric field strength inside the crack's tip	$E_\perp^{Cr}$	V m^{-1}
Saturation humidity	e_∞	g m^{-3}
Actual humidity	e_n	g m^{-3}
Humidity deficit	$e_n - e_\infty$	g m^{-3}
Diffusion coefficient of water vapor in the atmosphere	D	m^2 sec^{-1}
Electric potential	U	V
Density of ice	ρ_c	kg m^{-3}
Time of complete evaporation of an ice sphere	t	sec
Ambient electric field	E_0	V m^{-1}
Charge relaxation times	τ_1	s
Distance	d	m

particles measured with a Faraday cage[26] or by a special trap[27] represent only "secondary" residual charges. But although these highly energetic hotspots inside an ice media appear and disappear in fractions of seconds they can lead to chemical consequences. The closest analogy is possibly the activation of chemical reactions in liquids by ultrasonic radiation.[95]

3. Potential chemical processes caused by the electrical charging of snow and ice

In the following chapters we discuss potential chemical processes that can occur under natural conditions as a result of the electrical charging of ice.

3.1. Changes of pH

Charging of ice results from redistribution and local accumulation of charge carriers like H^+, OH^-, and Bjerrum defects, thus it can lead to pH changes with maximum changes at the previously described "hotspots" at the tips of a growing crystal or growing crack. Since ice is a highly dynamic system these changes are quite variable. The detachment of a charged fragment (Fig. 4) with excess of either H^+ or OH^- can result in a change of the pH value. Nelson and Baker,[16] who modelled ice microstructure changes during growth or sublimation, argued that charging during growth may make the ice surface more alkaline due to the enrichment of OH^-, while sublimation leads to an acidification. According to their estimates the tip of a growing ice crystal with a growth rate of 1 μm s^{-1} and a charge of 20 fC has a pH of 9.6.

3.2. Redox reactions

Redox reactions were used by Finnegan *et al.*[33] and Shavlov *et al.*[34,56] as a tool with the aim to detect the quite transient charging of growing ice boundaries. Finnegan *et al.*[61] studied the redistribution of charges in a growing ice crystal and demonstrated that such charging leads to the formation of so called "electric multipoles" (Fig. 3a). Such charging affects the ice crystal shape, the configuration of ice crystal aggregates (Fig. 3c), the rates of aggregation, and the formation of secondary ice crystals. Chemical reactions occurred rapidly during ice crystal growth in a supercooled liquid water cloud at −16 °C.[33] Sulfide was oxidized to sulfate, while halide ions were oxidized to higher valence ions in a coupled set of chemical reactions occurring simultaneously. The reduction of silver ions to elemental silver and of sulfate ion to lower valence species have also been documented.[33] Similar reactions have been reported to occur during the freezing of bulk dilute solutions of ammonium and/or halide salts.[33]

Shavlov *et al.*[34,56] also studied redox reactions in ice and theoretically examined the mechanism of ice charging during growth. They developed the idea of charging due to redistribution of main charge carriers in the ice further (*e.g.* (ref. 16, 42, 60 and 62)) (Ch. 2.3). Redox reactions were used with the aim to illustrate the electric activity of phase boundaries during growth. Shavlov *et al.*[34] showed that films of copper, aluminum, iron, and silver decreased their electrical conductivity in contact with growing ice due to corrosion.

Despite the experimental evidences in favor of the occurrence of redox reactions, it should be noted that Khusnatdinov and Petrenko[93] demonstrated that electrons cannot be charge carriers in ice. Thus, redox reactions can occur only on the ice boundaries.

3.3. Increased scavenging of aerosols, pollutants, and trace gases

Electric forces play a significant role in microscale aerosol scavenging along with other factors as thermo- and diffusiophoretic forces, Brownian diffusion, and inertial impaction.[96] The role of charging during growth in more effective collection of ions, aerosols, and droplets by ice was pointed out by Nelson and Baker.[16] Snowflakes are ∼28–50 times more effective in scavenging per equivalent water content compared to rain drops.[97–100] As a result of the combined effect of different factors the impact is especially large for the so-called Greenfield gap size (0.2–2 μm).[101] Such microscale aerosols are always charged, so in this case the role of electrostatic forces become comparable to the role of developed surface area and filtering ability due to porosity. Scavenging effectiveness due to electric forces of snowflakes and grounded growing objects such as frost flowers, hoarfrost, or rime depends on the average electric field strength (Ch. 2.7), humidity, and temperature conditions. Probably, the most effective scavengers are rapidly growing rime, hoar, and frost flower crystals with morphology and ambient conditions leading to corona discharges at their sharp tips (see below, Ch. 3.5), so that they can capture pollutants as effective as industrial electrostatic precipitators which remove 40 to 95% of the particles.[102]

3.4. Electro osmotic processes: redistribution of ions

Electric fields can stimulate electrophoretic migration of ions in a quasi-liquid layer on the surface of ice crystals or inside

capillaries. Like in capillary electrophoresis ion drift velocities depend on their charges, size, polarization ability, steric effects, and ions planarity[103,104] leading to similar processes of ion redistribution under the influence of an electric field. This can be important if the redistributed ion enters, for example, an electric field sufficient for a corona discharge.[36] As a result, the supply of various ions to the reaction zone proceeds at different rates. If the products of these reactions initiated by corona discharges trigger other free radical processes like the formation of reactive halogen species, the changes in the composition of the atmosphere above the snow can be significant.

3.5. Corona discharge: free radical processes

Corona discharges appear in regions with a high gradient of electric field as channels of energy dissipation.[105] Such discharges are microscopic and dissipate instantly, therefore, they will be difficult to observe under natural conditions. However, their impact may not be negligible.

Corona discharges occur when electric field overcomes the critical value of 10^6 V m^{-1} at standard pressure.[44–46] The charge accumulation can be the result of any of the processes discussed in Chapter 2. Under the influence of a corona discharge, molecules become excited and the degradation of the excited states leads to the formation of reactive species. OH$^\bullet$ radicals, H$^\bullet$, oxygen, and nitrogen atoms, and ozone can be formed from the atmospheric nitrogen, oxygen, and water vapor. H$^\bullet$ and nitrogen atoms undergo oxidation due to the presence of ozone and oxygen. Recombination of hydroxyl radicals can increase the concentration of hydrogen peroxide in the snow.

Under the influence of the corona discharge, organic compounds (for instance, persistent organic pollutant) can undergo degradation or chemical transformation. Thus, the occurrence of corona discharges in snow can result in increasing levels of NO_x, OH$^\bullet$, and O_3 and the transformation of persistent organic pollutants (POPs). However, since corona discharges persist only a fraction of a second, only conditions that stimulate a strong electrification of the snow (extremely low temperatures, low humidity, high wind speeds) offer the possibility to incur visible changes of the concentration of these compounds.

The strongest impact of such intermittent radical formation can be expected if they trigger chain reactions leading to a detectable impact on major trace gases. The most prominent example is potentially the complete destruction of boundary layer ozone in polar regions mainly occurring during springtime,[106] which are regularly accompanied by a comparable depletion of atmospheric mercury.[107] The depletion is driven by radical reactions involving reactive bromine species, likely accompanied by reactive chlorine and iodine compounds.[106,108] While the radical reaction mechanism leading to the effective destruction of ozone is well known (*e.g.* (ref. 106, 109 and 110)), the processes leading to the initial formation and the efficient recycling of bromine radicals are still under debate. Here, corona discharge processes may also contribute to the activation of bromine species since bromide is omnipresent in natural snow in polar regions (*e.g.* (ref. 106 and 111)). In fact, radical formation due to corona discharges may also be possible under conditions, which are often discussed as limiting the bromine radical formation and recycling. This concerns limiting factors related to the pH as well as solar radiation. The traditional bromine radical formation processes require acidic conditions since protons are directly involved in the heterogeneous reaction of HOBr with Br^- (or Cl^-), which is a key step in the formation of reactive halogens.[106] However, the formation of reactive bromine species in corona discharges are likely independent of pH values. Moreover, since the ozone depletions are traditionally observed during springtime after polar sunrise the reaction mechanisms mainly rely on photolytic reactions. Nevertheless, a limited number of observations also exist demonstrating a partial depletion of ozone and mercury already during dark conditions (*e.g.* (ref. 112 and 113)) (Ch. 4.5). Due to the widespread nature of the depletion of tropospheric ozone for example over the Arctic Ocean[114,115] it appears unlikely that radical formation due to electrical charging of snow and ice are always at the origin of the formation of the involved radical species. Nevertheless, a substantial contribution especially during the initial formation of halogen radicals cannot be excluded and should be considered in the further analysis of such events.

3.6. Aerosol production events

Maximum charge values according to our estimates occur when different factors act together: at the tip of a grounded conductor in a strong electric field under the influence of wind (Ch. 2.9, Table 2). Overcoming of the Rayleigh limit[90,91] is followed by "spraying" of aerosol submicron particles known as Rayleigh jets.[69,92] These highly-charged sub-micrometer aerosols can also dissipate the energy through free radical processes and redox reactions.

This phenomenon has been widely investigated in laboratory experiments aimed at understanding atmospheric electricity processes.[69,116–119] The overcoming of the Rayleigh limit can lead to avalanche-like aerosol formation events, well known under natural conditions (Ch. 4.4).

The phenomenon of charged particles being ejected from droplets under high electric potential is used in electrospray ionization mass-spectrometry to produce gas-phase ions.[120] Charged micro-droplets in Rayleigh jets decrease in size as a result of solvent evaporation until they reach the Rayleigh limit and break up again. This disintegration process continues until the formation of molecular ions. Sharp grounded objects like frost flowers concentrate electric field on their tips and, so they can act like emitters in electrospray mass spectrometry[36] (Fig. 7) potentially leading to the direct transfer of bromine or iodine ions from the condensed to the gas phase with the following initiation of ozone depletion.[36]

4. Influence of different charging mechanisms on snow chemistry processes

In this chapter we aim to point out field observations of the chemical composition of natural snow and ice like frost flowers and chemical processes related to the interaction of snow and the atmosphere, which are hitherto unexplained or difficult to explain without considering electrostatic

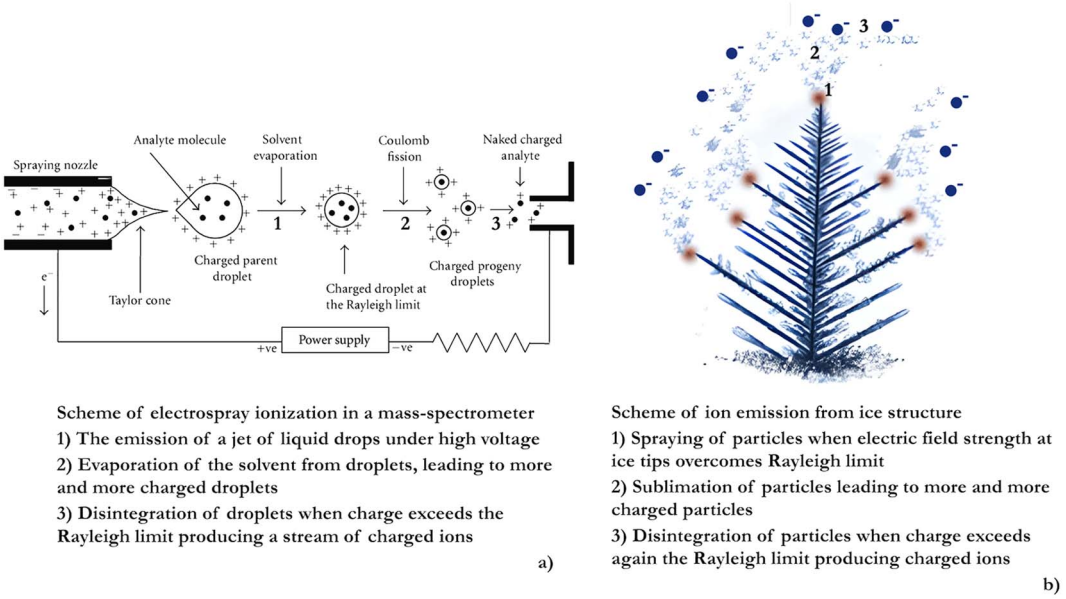

Fig. 7 (a) Scheme of an electrospray mass spectrometer (reproduced from ref. 121 with permission from Hindawi, copyright 2012); (b) mechanism of aerosol production by FF similar to the principle of electrospraying in mass-spectrometry (reproduced from ref. 36 with permission from Elsevier, copyright 2017).

processes. The following sub-chapters are sorted according to the above described processes leading to electrical charges in snow and ice. In each chapter we focus on selected publications by describing in detail which observation may be related to one of the above described chemical process.

4.1. Charging due to growth. Enrichment of growing crystals with mercury and different impurities

Despite being far from sources, mercury and persistent organic pollutants occur in both polar regions.[122,123] Moreover, mercury and POPs can be enriched in the various elements of the cryosphere (snow, glaciers, sea ice, *etc.*). Douglas *et al.*[6] performed field experiments near Barrow, Alaska to measure mercury concentrations in different ice and crystal types. The highest concentration of mercury (15 500 ng l^{-1}) was found in rime that formed during a few seconds on the wings of a drone flying over a sea ice lead. Concentrations in further rime samples formed during other experiments were also consistently high (1580 ng l^{-1} and 5200 ng l^{-1}). In diamond dust and surface hoar samples, mercury concentrations of up to 1370 ng l^{-1} and between 41 and 975 ng l^{-1} were found. These observations indicate that the accumulation of mercury in the ice crystals is potentially driven by highly charged ice crystals tips, which facilitate the uptake of the polarizable mercury atom. As demonstrated in Chapter 2.3 higher growth rates lead to a stronger accumulation of charges in the tips of the growing ice crystals in agreement with the observed concentrations in the different crystal types.

Frost flowers are also characterized by strong growth rates and should, thus, exhibit high mercury concentrations possibly comparable to surface hoar. However, the frost flower samples collected by Douglas *et al.*[6] at comparable conditions only showed mercury concentrations up to 180 ng l^{-1}. Nevertheless, Douglas *et al.*[124] reported previously mercury concentrations of about 820 ng l^{-1} in frost flowers collected near a sea ice lead, which were affected by high humidity gradients due to convective plumes above the open water. These meteorological conditions, may have contributed to a faster growth rate of these frost flowers and, thus, contributed to the enrichment of the frost flowers in mercury.

In general, frost flowers can be regarded as grounded conductors (Ch. 2.7 and 3.3), which are analogues of lightning rods, which can capture impurities from the atmosphere as effective as industrial electrostatic precipitators due to their charged tips. This hypothesis is an agreement with the observations by Sherman *et al.*[125] They studied frost flowers during their growth and determined that the concentrations of major anions and cations in the ice crystals decreased due to the addition of water vapor from the gas phase, while at the same time mercury concentrations increased from 128–164 ng l^{-1} in the dry frost flower to 200 ng l^{-1} during a period of 48 h.[125] Such an increase can be explained by the continuous and enhanced absorption of mercury from the gas phase due to the charging of the crystal tips.

The charging of ice and snow has so far not been considered for the transfer of mercury from the gas phase to the cryosphere. Similar to atmospheric mercury depletion events, which occur mostly in springtime,[107] it would increase the deposition of mercury to ice and snow in polar regions. However, electrical charging can occur year-round with a stronger effect likely in the freezing periods in fall and winter. The deposited mercury subsequently enters the marine and terrestrial ecosystems, where it acts as a toxic agent and can further be enriched due to abiotic and biotic processes. Therefore, it would be important to determine the role of charging process in the deposition of

mercury in polar regions. The same mechanism can also contribute to the enrichment of other impurities, which were found at high levels in frost flowers as well as in rimed snow and ice that usually show higher concentrations of POPs and other impurities[126] than other types of deposited snow.[3,127,128] Soluble atmospheric trace gases are also accumulated by ice during riming (*e.g.* sulfur dioxide, hydrogen peroxide, ammonia, nitric acid, formaldehyde, formic acid, hydrogen chloride).[6,129,130]

Enhanced scavenging processes[131] as well as emission of iodine[132] have been observed close to lead. These phenomena are poorly understood yet. Since leads create high humidity gradients it can be assumed that they stimulate the ice crystal growth, and also contribute to fog, which decreases the air conductivity[77] resulting in an increased ambient electric field E_0. Both effects lead to an enhanced electric field strength E on the growing tips of the frost flowers (Ch. 2.7).

4.2. Blowing snow events: friction, cracking, and sublimation

Blizzard offers a combination of all factors mentioned above (Chapter 2) of snow charging due to an efficient grinding and breaking of snow grains. Turbulent mass transfer leads to continuous removal of vapor-saturated masses with their replacement by drier air. This moisture deficit stimulates sublimation and growth inside the snowpack (*e.g.* (ref. 83 and 84)). Friction gives highest values of charging under low temperatures, low humidity, and high friction velocities, *i.e.* under high wind speeds (Ch. 2.2). Therefore, the strongest triboelectrification during blizzards is likely to occur in the interior of the Antarctic continent with temperatures in the range from −30 to −70 °C.[133] So-called katabatic winds are a source of a dense cold air flowing down towards coastal areas, where they can merge with cyclonic flows to generate hurricanes with wind speeds of 50 to 60 m s^{-1}, rarely reaching peaks on the order of 90 m s^{-1}.[133] The Antarctic stations like Mirniy and Molodezhnaya encounter storms more often than 200 days per year, while the Mawson station even registers storms on more than 300 days per year.[133]

Remote locations in the interior of the Antarctic continent or on the Greenland ice sheet are also characterized by clean snow with small concentrations of impurities. Since the thickness of the ice sheets prevents charge dissipation, they can be considered as a snow cloud with processes inside very similar to clouds. In this case, the snow cover is permeable for the electric field that appears during blizzards, which can strongly accelerate metamorphism processes inside the snowpack. It can, thus, be expected that these periods are prone to significant chemical transformations, which were observed during previous field experiments.

Hydroxyl radicals ($OH^{\bullet}$) play a key role in controlling the oxidizing power of the troposphere.[134] Inland polar locations, such as South Pole and Summit (central Greenland), were found to have surprisingly high atmospheric concentrations of $OH^{\bullet}$ radicals, comparable to those encountered in the tropics ($(3–6) \times 10^6$ cm^{-3}).[135] At these inland stations the $OH^{\bullet}$ concentration were about 5 times higher than its levels measured at coastal stations. Further studies have indicated that photochemical reactions linked to the participation of HCHO,[136,137] NO_x,[138] HONO,[139,140] hydrogen peroxide,[141] higher aldehydes,[142] and HO_2 radicals[143] in the snow-atmosphere continuum contributed to these elevated $OH^{\bullet}$ levels.[144] However, in a number of cases it became obvious that simulated $OH^{\bullet}$ levels using only photochemical reactions in the snow and the atmosphere underestimated the observed values.[7] Moreover, this discrepancy between modelled and measured values was strongly dependent on meteorology. According to Sjostedt *et al.*[7] when the wind speeds were low (<6 m s^{-1}) the measured values were already two times higher than the calculated values, whereas at high wind speeds (>6 m s^{-1}) and blowing snow the OH levels increased even further. Under these conditions the observed values were approximately an order of magnitude higher than the simulated OH values.[7] Such an additional production of the OH radical can be caused by the processes presented in Ch. 2.9 at Summit, which offers favourable conditions for the charge accumulation on snow grains due to tribo-processes such as friction, cracking and intensive sublimation caused by high wind speeds. If charges accumulated on the crystal surfaces overcome the corona threshold value, the free radical decomposition of water molecules will for example result in the production of OH radicals.

4.3. Electric field generated by blizzards can stimulate charging due to metamorphism. NO_x production inside the snowpack

Due to its porous nature, snow covers represent complex multiphase systems (*e.g.* (ref. 3)). In this system, the interstitial air, which is trapped within the gaps between the snow crystals, creates a porous and open framework. Since the interstitial air is connected to the atmosphere as well as closely linked to the surface of the snow crystals and processes therein, it is a crucial component for snow-atmosphere interaction. As a result, the composition of the interstitial air is related to processes and interactions with the snow crystals and exhibits often significantly different concentrations compared to ambient air (*e.g.* (ref. 145 and 146)). The interstitial air is further characterized by strong vertical gradients for example in temperature[86] and radiation.[147] While a number of observed elevated concentrations in the interstitial air close to the surface of the snow cover on the ice sheets in Greenland and Antarctica can be explained by photochemical reactions,[145] observations of elevated ozone and NO_x concentrations in the dark (*e.g.* during shading experiments or in layers down to 2 m depth[8,146,148,149]) remain unexplained. The role of wind has been evoked in previous studies,[8,148] while its role in the NO_x production in the dark is still not clear.[8] More recent data demonstrate that the formation of NO_x in the interstitial air of the snow cover on top of the Antarctic ice sheet is possible even during the winter. Due to the high permeability of the snow cover for electric fields generated at the surface of the snow cover by blizzards, these fields can also influence deeper layers of the snow, where they can contribute to fast metamorphism processes favored by high

temperature and humidity gradients as described in Ch. 2.8 and potentially leading to the formation of NO_x due to enhanced radical reactions.[8]

4.4. Wind-induced formation of charged aerosols

High wind speeds can create conditions to overcome the Rayleigh limit (Ch. 3.6) forming Rayleigh jets of charged nanoparticles. Virkkula *et al.*[150] measured from December 2004 to January 2005 at the Finish Antarctic station Aboa the charges of aerosols particles and the concentrations of ions to study the role of ions as nucleating particles for the formation of secondary aerosols. They focused on concentrations of two aerosols fractions: so-called "cluster ion" corresponding to clusters of ions and particles with diameters less than 1.6 nm and "intermediate ion" corresponding to particles with diameters between 1.6 and 8 nm. During the most representative days with particle formation intermediate ion concentrations increased approximately two orders of magnitude and more negative than positive intermediate ions were observed. The processes described in Chapter 3.6 lead for example to a preferred formation of negative aerosols by charged grounded objects, which are always negatively charged (Chapter 2.7). During wind-induced particle events a correlation between wind speed, clusters of ions, and intermediate ions was observed.[150] This effect was seen at wind speeds higher than 15 m s^{-1} for intermediate ions. During wind-induced particle formation events at wind speeds higher than 20 m s^{-1} the ratio between positive and negative cluster ion concentrations was close to 1. This can be the result of the charging of snow drifting particles (Chapter 2.9) above the Rayleigh limit, resulting in the formation of negatively and positively charged particles. In line with the here proposed processes in the snow, Virkkula *et al.*[150] also observed a dramatic increase of ion concentrations of up to 1000 cm^{-3} at the beginning of a snow storm. These authors hypothesized that charged aerosol formation processes can result from charging under the influence of high wind speeds and can be similar to processes in cumulonimbus clouds.

4.5. Reactive halogen production in polar regions during dark periods

Reactive halogens have attracted a lot of attention due to their role in the destructions of tropospheric ozone, the disturbance of radical cycles, and the oxidation of gaseous elemental mercury in both polar regions.[151] However, there are still many open questions about the initiation of these periods of depleted ozone and mercury, which can last for variable periods. The destruction of ozone is mainly driven by reactive bromine, which undergoes an exponential increase in the involved photochemical reaction cycles causing the so-called "bromine explosion". However, it is still under debate how the initial "seed" bromine[151] for these destruction cycles is created from the omnipresent marine bromide. Highly charged ice and snow surfaces generated in processes described in Ch. 2 have the potential to contribute to the initial halogen production through corona initiated free radical reactions (Ch. 3.5).

Moreover, a number of observations also point to the formation of reactive halogen compounds already during dark conditions, which do not support photochemical reaction pathways. Already in 2001, Foster *et al.*[152] reported elevated quantities of Br_2 and BrCl at Alert, Canada right at the time of polar sunrise, which indicate that the formation already started during the dark period. Simpson *et al.*[113] reported "unprecedented levels" of BrO of up to 90 pmol mol^{-1} in air masses soon after polar sunrise in February 2017 at Utqiaġvik, Alaska. While the tropospheric vertical column density of BrO reached 1.3 × 10^{14} molecules cm^{-2}, the back-trajectory analysis demonstrated that the high BrO levels occurred in airmass originating from higher latitudes characterized by near total darkness and, thus, minimum prior photochemistry. Such high levels of BrO may be the result of the built-up of highly photolabile bromine species like Br_2 or BrCl produced by night-time formation mechanism due to electrical charging of snow and ice.

Finally, Nerentorp Mastromonaco *et al.*[112] observed depleted ozone and mercury during the winter period in Antarctica in air masses coming from dark regions. They also proposed a previous built-up of Br_2 that was possibly formed in high concentrations in the marine boundary layer in the dark. With elevated concentrations of this precursor the incoming radiation at large solar zenith angles is sufficient to initiate the photolytic formation of halogen radicals and the observed destruction of ozone and mercury.

5. The way forward

To confirm the importance of the above described chemical processes in ice and snow further laboratory experiments and field studies are required. Laboratory experiments can likely build on approaches that were already used with the aim to study ice charging. Such experiments could be upgraded to include also chemical measurements. For example, experiments for the growth of ice dendrites causing the detachment of tip fragment and its flight attracted by a film of a polar liquid, so called 'electrostatic jumping of frost' (57, see Ch. 2.3) or spraying of microparticles from growing sharp ice tips under the influence of an electric field[16] could also include chemical measurements of the fragments or the microparticles since modern analytical instruments only require small sample volumes. A further possibility may be laboratory experiments of artificial or natural snow under conditions leading to strong metamorphism (*e.g.* (ref. 153)) or strong mechanical stresses (*e.g.* (ref. 154)). Artificial snow offers the advantage to better control the chemical concentrations and to limit the number of potential reactants using doped snow (*e.g.* (ref. 155–158)). Such experiments will have in common to study potential products of chemical processes induced by electrical charges. However, observing the formation of reactive species *in situ* due to electrical charges will require non-invasive, remote sensing techniques. However, these are currently probably to limited to detect the described small-scale processes with their likely transient features. To overcome such limitations, the snow could further be doped with compounds trapping radicals like previously applied in studies for liquid phase reactions (*e.g.* (ref.

159 and 160)). To augment the effect of electrical charges, the snow and ice samples in such experiments could further be exposed to variable external electric fields and/or UV radiation. Such a set-up could potentially be useful for the study of the fate of POPs in charged ice media, which can eventually deliver relevant results concerning the fate of these compounds in polar regions. Similarly, the motion of ions in ice media due to electric fields (electrophoresis) maybe made visible by fluorescent dyes.

Future field studies integrating approaches as described above would also be of interest. Since periods with high wind speeds and low temperatures are most favorable for the charging of snow and ice, the most promising location to perform successful field experiments is the Antarctic plateau, where snow storms are common. Nevertheless, coastal or marine regions either in the Arctic or Antarctic are also promising locations to encounter such phenomena especially in winter and may deliver further results due to the higher chemical load of the snow and ice including inorganic and organic species at these locations. Areas with intensive and fast sea ice growth like coastal polynyas could also be interesting targets for field experiments. The dark winter period should be aimed to perform such experiments to exclude parallel processes induced by photochemical reactions. During field work it would be of interest to measure the electric field at the tip of a growing ice crystal also with non-invasive techniques. Since blowing snow creates differently charged snow particles, a further option could be to collect these charged snow particles separately to analyze if they exhibit differing chemical compositions due to processes occurring in the differently charged particles.

6. Summary and conclusions

Electrical charging of ice crystals in clouds manifest themselves in different atmospheric electricity phenomena and can be sufficient to initiate chemical reactions, such as nitrogen oxide production from atmospheric nitrogen.[32] Some mechanisms of ice charging in clouds occur as well at sea level. In the present review such processes as friction, cracking, sublimation and condensation growth are discussed and the strength of the electrical fields that can be achieved at sea level are estimated for each process based on literature data on ice physics. If multiple mechanisms act together, higher field strengths can be achieved.[17,65–68] Comparable to atmospheric processes in clouds, which can lead to the formation of strong electric fields, processes occur in the snowpack under the influence of a blizzard. It stimulates not only the electrification of ice particles due to tribo-electric processes such as rubbing and cracking but also due to the intensification of ice sublimation and growth.[87] Overall, electric phenomena in snow and ice and their importance for chemical processes has so far received little attention. However, they have the potential to contribute to some observations that have remained so far unexplained.

The combined effect of different mechanisms can lead to overcoming the threshold of the field strength that is required for the appearance of the corona discharge. Such corona discharges occur and dissipate in microseconds like "hotspots" inside an ice media[68] and have the potential to stimulate molecules in the zone of their influence with the subsequent formation of active species such as radicals. Under these conditions, activation of atmospheric nitrogen, oxygen, and water vapor results in increasing levels of NO_x, $OH^{\bullet}$, H_2O_2, and O_3. However, if in marine regions radicals like halogens are formed that are involved in catalytic cycles leading to the destruction of ozone, the impact of corona discharge processes is strongly amplified. Furthermore, organic compounds and POPs can undergo degradation or chemical transformation due to the postulated corona discharges.

The mechanism of charge accumulation on the tips of grounded ice structures such as frost flowers are also presented with estimates of the corresponding electric field strengths, which can be achieved at their tips under different conditions. Frost flowers under fair weather conditions are good examples of grounded ice objects close to the bifurcation point, where even small changes in meteorological and environmental conditions can result in achieving the threshold for the appearance of corona discharges. This threshold can be achieved by many different ways. The key parameter that allows corona discharges is the electric field strength on the growing frost flower tip, which depends on the combined effects of many meteorological and environmental factors. The radius and the length of the ice crystal's tip depend on temperature and humidity conditions during the growth of the crystal. If the ice tip radius has the size of about a few μm, even small changes in the terrestrial electric field strength due to diurnal or seasonal variations or other environmental conditions like the presence of a sea ice lead or the occurrence of geomagnetic storms can turn the corona discharge on or off. UV light is a further factor that can strongly increase the possibility of reaching the threshold for a corona discharge, because UV irradiation increases the quantity of charge carriers[93] leading to a higher level of charging. However, since UV radiation can also initiate photochemical reactions in snow it appears impossible that only the effect of electric phenomena without any contribution from photochemistry can be observed under daytime natural conditions. Nevertheless, if the snow initially undergoes photoirradiation, its electrification during a blizzard is likely higher and the potential that the electric field strength overcomes the threshold value for the corona discharge under moderate winds is higher in spring and summer due to the impact of the UV radiation on snow electrification.

During extreme conditions like in blizzards the field strengths can even pass the Rayleigh limit[90,91] leading to the "spraying" of sub-micro particles known as Rayleigh jets.[69,92] The particles that are ejected during such events are charged. These submicron particles decrease in size as a result of sublimation until they reach the Rayleigh limit and break apart again. This disintegration process can continue until the formation of single charged particles similar to molecular ions as in electrospray mass spectrometry.[91] Thus, it can be assumed that some ions can be emitted into the atmosphere. For instance, this may be a mechanism of the direct transfer of

bromine or iodine ions from the condensed to the gas phase with the following initiation of ozone depletion.

But even if the electric field strength remains lower than the above mentioned thresholds, some changes in the chemical composition of ice and snow may occur. Since charging can stimulate the attraction and assimilation of charged particles, polarized, and polarizable molecules from the atmosphere, rime, hoar, and frost flowers can effectively collect ions, aerosols, and droplets[16] analogue to electrostatic precipitators. This may explain elevated levels of mercury and other impurities in freshly formed hoar, rime, and frost flowers.[124–126] Such processes may be relevant for the behavior of pollutants in the cryosphere with important environmental implications for polar or high-altitude regions.

Each snow flake and each growing or sublimating ice crystal is polarized[61] and this charging is quite variable as it is influenced by environmental conditions. The snow pack is a highly variable electrodynamic system.[89] Considering these electric phenomena remains a complex task since direct observations are still very limited and remain difficult to perform. To overcome these limitations, we presented some ideas for new laboratory experiments and field observations that may contribute to provide evidence of the impact of electric phenomena. Most promising for such experiments are high-elevation sites in the interior of the Antarctic continent or on the Greenland ice sheet with highly pure snow, high wind speeds, low temperatures, and low atmospheric pressure, which decreases the corona threshold.[44–46] To avoid the impact of photochemical process, observations during the polar night will be most valuable to identify the impact of the described electric phenomena.

The aim of the review is to draw attention to this new field integrating ice physics and snow chemistry and to stimulate further actions in this direction. Currently, the two considered topics are treated by disconnected communities. The objective is to draw these communities closer together to create a common interest and to initiate new cooperation leading to novel and innovative research contributing to a better understanding of chemical processes related to the vulnerable terrestrial cryosphere.

Author contributions

KT developed the idea of this review and created the images. KT and HWJ developed the concept of the review, performed the data and literature analysis, collected evidence, and wrote the manuscript.

Conflicts of interest

There are no conflicts to declare.

Acknowledgements

The study was financed by the National Academy of Science of Ukraine, grant 0120U100574, and the State Ukrainian Program of Research in Antarctica. We also acknowledge support by the College de France in the frame of the Program PAUSE and by the Université Grenoble Alpes. We are also grateful to Oleg Varzatskii and Sergey Kozachkov for advice and fruitful discussions.

References

1 R. E. Honrath, M. C. Peterson, S. Guo, J. E. Dibb, P. B. Shepson and B. Campbell, Evidence of NO_x production within or upon ice particles in the Greenland snowpack, *Geophys. Res. Lett.*, 1999, **26**, 695–698.

2 A. M. Grannas, A. E. Jones, J. Dibb, M. Ammann, C. Anastasio, H. J. Beine, M. Bergin, J. Bottenheim, C. S. Boxe, G. Carver, G. Chen, J. H. Crawford, F. Dominé, M. M. Frey, M. I. Guzmán, D. E. Heard, D. Helmig, M. R. Hoffmann, R. E. Honrath, L. G. Huey, M. Hutterli, H.-W. Jacobi, P. Klán, B. Lefer, J. McConnell, J. Plane, R. Sander, J. Savarino, P. B. Shepson, W. R. Simpson, J. R. Sodeau, R. von Glasow, R. Weller, E. W. Wolff and T. Zhu, An overview of snow photochemistry: evidence, mechanisms and impacts, *Atmos. Chem. Phys.*, 2007, **7**, 4329–4373.

3 T. Bartels-Rausch, H.-W. Jacobi, T. F. Kahan, J. L. Thomas, E. S. Thomson, J. P. D. Abbatt, M. Ammann, J. R. Blackford, H. Bluhm, C. Boxe, F. Domine, M. M. Frey, I. Gladich, M. I. Guzmán, D. Heger, Th. Huthwelker, P. Klán, W. F. Kuhs, M. H. Kuo, S. Maus, S. G. Moussa, V. F. McNeill, J. T. Newberg, J. B. C. Pettersson, M. Roeselová and J. R. Sodeau, A review of air–ice chemical and physical interactions (AICI): liquids, quasi-liquids, and solids in snow, *Atmos. Chem. Phys.*, 2014, **14**, 1587–1633.

4 R. Röthlisberger, M. A. Hutterli, E. W. Wolff, R. Mulvaney, H. Fischer, M. Bigler, K. Goto-Azuma, M. E. Hansson, U. Ruth, M.-L. Siggaard-Andersen and J. P. Steffensen, Nitrate in Greenland and Antarctic ice cores: A detailed description of post-depositional processes, *Ann. Glaciol.*, 2002, **35**, 209–216.

5 M. Legrand, S. Preunkert, J. Savarino, M. M. Frey, A. Kukui, D. Helmig, B. Jourdain, A. E. Jones, R. Weller, N. Brough and H. Gallée, Inter-annual variability of surface ozone at coastal (Dumont d'Urville, 2004–2014) and inland (Concordia, 2007–2014) sites in East Antarctica, *Atmos. Chem. Phys.*, 2016, **16**, 8053–8069.

6 T. A. Douglas, M. Sturm, W. R. Simpson, J. Blum, L. Alvarez-Aviles, G. J. Keeler, D. K. Perovich, A. Biswas and K. Johnson, Influence of snow and ice crystal formation and accumulation on mercury deposition to the Arctic, *Environ. Sci. Technol.*, 2008, **42**, 1542–1551.

7 S. J. Sjostedt, L. G. Huey, D. J. Tanner, J. Peischl, G. Chen, J. E. Dibb, B. Lefer, M. A. Hutterli, A. J. Beyersdorf, N. J. Blake, D. R. Blake, D. Sueper, T. Ryerson, J. Burkhart and A. Stohl, Observations of hydroxyl and the sum of peroxy radicals at Summit, Greenland during summer 2003, *Atmos. Environ.*, 2007, **41**(24), 5122–5137.

8 B. Van Dam, D. Helmig, C. Toro, P. Doskey, L. Kramer, K. Murray, L. Ganzeveld and B. Seok, Dynamics of ozone

and nitrogen oxides at Summit, Greenland: I. Multi-year observations in the snowpack, *Atmos. Environ.*, 2015, **123**, 268–284.
9 P. Lenard, Über die Electricität der Wasserfälle, *Ann. Phys.*, 1892, **282**(8), 584–636.
10 P. Lenard, Über Wasserfallelektrizität und über die Oberflächenbeschaffenheit der Flüssigkeiten, *Ann. Phys.*, 1915, **352**(12), 463–524.
11 G. C. Simpson, The mechanism of thunderstorm, *Philos. Trans. R. Soc., A*, 1909, **209**, 379.
12 H. Tammet, U. Hõrrak and M. Kulmala, Negatively charged nanoparticles produced by splashing of water, *Atmos. Chem. Phys.*, 2009, **9**, 357–367.
13 J. K. Lee, K. L. Walker, H. S. Han, J. Kang, F. B. Prinz, R. M. Waymouth, H. G. Nam and R. N. Zare, Spontaneous Generationof Hydrogen Peroxide from Aqueous Microdroplets, *Proc. Natl. Acad. Sci. U. S. A.*, 2019, **116**(39), 19294–19298.
14 M. A. Mehrgardi, M. Mofidfar and R. N. Zare, Sprayed Water Microdroplets Are Able to Generate Hydrogen Peroxide Spontaneously, *J. Am. Chem. Soc.*, 2022, **144**(17), 7606–7609.
15 J. Latham, Electrification produced by the asymmetric rubbing of ice on ice, *Br. J. Appl. Phys.*, 1963, **14**, 488–490.
16 J. Nelson and M. Baker, Charging of ice-vapor interfaces: applications to thunderstorms, *Atmos. Chem. Phys.*, 2003, **3**, 1237–1252.
17 E. E. Avila and G. M. Caranti, A laboratory study of static charging by fracture in ice growing by riming, *J. Geophys. Res.*, 1994, **90**(D5), 10611–10620.
18 G. C. Simpson and British Antarctic expedition, *1910–1913: Meteorology*, Thacker, Spink & Co., Calcutta, India, 1919, vol. 1, p. 326.
19 P. C. Pearce and B. W. Currie, Some qualitative results on the electrification of snow, *Can. J. Res.*, 1949, **27**(1), 1–8.
20 V. J. Schaefer, Properties of particles of snow and the electrical effects they produce in storms, *Trans., Am. Geophys. Union*, 1947, **28**(4), 587–614.
21 C. Magono and N. Sakurai, On the electric charge on drifting snow pellets, *J. Meteorol. Soc. Jpn.*, 1963, **41**(4), 211–217.
22 J. Latham, The electrification of snowstorms and sandstorms, *Q. J. R. Meteorol. Soc.*, 1964, **90**(383), 91–95.
23 J. R. Herman, Precipitation static and electrical properties of blowing snow at Byrd Station, Antarctica, in *Geomagnetism and Aeronomy: Studies in Ionosphere, Geomagnetisme and Atmospheric Radio Noise, Antarctic Research Series*, ed. A. H. Waynick, Wiley, American Geophysical Union, 1965, vol. 4, pp. 221–236.
24 J. Latham and C. D. Stow, Electrification of blowing snow, *J. Meteorol. Soc. Jpn.*, 1965, **43**(1), 23–29.
25 J. Latham and J. Montagne, The possible importance of electric forces in the development of cornices, *J. Glaciol.*, 1970, **9**(57), 375–384.
26 E. R. Wishart, Electrification of Antarctic Drifting Snow, in *Proceedings Int. Symposium Antarctic Glaciological Exploration*, IASH Publ, Hanover, NH: USA, 1970, vol. 86, p. 316.
27 D. S. Schmidt, R. A. Schmidt and J. D. Dent, Electrostatic force in blowing snow, *Boundary Layer Meteorol.*, 1999, **93**, 29–45.
28 M. Gordon, S. Biswas, P. A. Taylor, J. Hanesiak, M. Albarran-Melzer and S. Fargey, Measurements of drifting and blowing snow at Iqaluit, Nunavut, Canada during the STAR project, *Atmos.-Ocean*, 2010, **48**, 81–100.
29 Y. Yair, Y. Reuveni, S. Katz, C. Price and R. Yaniv, Strong electric fields observed during snow storms on Mt. Hermon, Israel, *Atmos. Res.*, 2019, **215**, 208–213.
30 M. Lehning, J. Doorschot, N. Raderschall and P. Bartelt, Combining snow drift and SNOWPACK models to estimate snow loading in avalanche slopes, in *Snow Engineering 2000: Recent Advances and Developments*, ed. E. Hjorth-Hansen, London, 2000, pp. 113–122.
31 R. Bintanja, The contribution of snowdrift sublimation to the surface mass balance of Antarctica, *Ann. Glaciol.*, 1998, **27**, 251–259.
32 F. Leblanc, K. L. Aplin, Y. Yair, R. G. Harrison, J. P. Lebreton and M. Blanc, *Planetary Atmospheric Electricity*, Springer, Dordrecht, 2008, p. 534.
33 W. G. Finnegan, R. L. Pitter and L. G. Young, Preliminary study of coupled oxidation-reduction reactions of included ions in growing ice crystals, *Atmos. Environ.*, 1991, **25**(11), 2531–2534.
34 A. V. Shavlov, A. D. Pisarev and A. A. Ryabtseva, Corrosion of Metal Films in Ice: the Dynamics of the Conductivity of Films, *Russ. J. Phys. Chem. A*, 2007, **81**(7), 1030–1034.
35 E. Y. Tkachenko and S. G. Kozachkov, Possible contribution of triboelectricity to snow–air interactions, *Environ. Chem.*, 2012, **9**(2), 109–115.
36 E. Y. Tkachenko, Possible role of electric forces in bromine activation during polar boundary layer ozone depletion and aerosol formation events, *Atmos. Res.*, 2017, **196**, 1–7.
37 E. Tkachenko, Electrostatic mechanism of bromine release during ozone depletion events, *Ukr. Antarct. J.*, 2012, **10–11**, 128–135.
38 K. G. Libbrecht, The physics of snow crystals, *Rep. Prog. Phys.*, 2005, **68**, 855–895.
39 V. Sanin, *Newcomer in Antarctic*, Molodaya gvardiya, Moskva, 1973, p. 368, (in Russian).
40 P. R. Camp, Charge, morphology, and pH of natural snow, *J. Geophys. Res.*, 1976, **81**(9), 1589–1592.
41 V. M. Moochnik, *The Physics of Thunderstorm*, Gidrometeoizdat, Leningrad, 1974 (in Russian).
42 V. F. Petrenko, *Electromechanical Phenomena in Ice, Cold Regions Research & Engineering Laboratory Special Report 96-2*, Thayer School of Engineering Dartmouth College, USA, 1996.
43 Y. Yair, Charge Generation and Separation Processes, *Space Sci. Rev.*, 2008, **137**, 119–131.
44 R. F. Griffiths and J. Latham, The emission of corona from falling drops, *J. Meteorol. Soc. Japan*, 1972, **50**, 416–422.
45 C. N. Richards and G. A. Dawson, The hydrodynamic instability of water drops falling at terminal velocity in vertical electric fields, *J. Geophys. Res.*, 1971, **76**, 3445–3455.

46 D. A. Petersen, Laboratory study of electrical discharges on vapor grown ice crystals subjected to strong electric fields, PhD thesis, University of Nevada, Reno, 2009.
47 A. A. Shibkov, M. A. Zheltov and A. A. Korolev, Pulsed electromagnetic and acoustic emission accompanying fast crystallization of supercooled water droplets, *Vestn. Tambov. Gos. Univ., Ser. Estestv. Tekh. Nauki*, 2001, **6**(2), 162–169.
48 J. Latham and B. J. Mason, Electric charge transfer association with temperature gradients in ice, *Proc. R. Soc. London*, 1961, **260**(1303), 523–536.
49 J. Latham and C. D. Stow, A laboratory investigation of the electrification of snowstorms, *Q. J. R. Meteorol. Soc.*, 1967, **93**, 55.
50 P. V. Hobbs, *Ice Physics*, Clarendon Press, Oxford, 1st edn, 1974.
51 V. F. Petrenko and S. C. Colbeck, Generation of electric fields by ice and snow friction, *J. Appl. Phys.*, 1995, **77**(9), 4518–4521.
52 *2018 CODATA Value: Vacuum Electric Permittivity, the NIST Reference on Constants, Units, and Uncertainty*, 2019.
53 W. Findeisen, On the origin of storm electricity, *Meteorol. Z.*, 1940, **57**(6), 201–215.
54 T. Takahashi, Electrification of growing ice crystal, *J. Atmos. Sci.*, 1973, **30**, 1220–1224.
55 Y. Dong and J. Hallett, Charge separation by ice and water drops during growth and evaporations, *J. Geophys. Res.*, 1992, **97**(D18), 20361–20371.
56 A. V. Shavlov, V. A. Dzhumandzhi and A. A. Yakovenko, Charge Separation at the Evaporation (Condensation) Front of Water and Ice. Charging of spherical Droplets, *Tech. Phys.*, 2018, **63**(4), 482–490.
57 R. Mukherjee, S. F. Ahmadi, H. Zhang and R. Qiao, J.B. Boreyko Electrostatic jumping of frost, *ACS Nano*, 2021, **15**(3), 4669–4677.
58 N. Bjerrum, Structure and Properties of Ice, *Science*, 1952, **115**(2989), 385–390.
59 N. Maeno, *The Science of Ice*, Hokkaido University Press, 1981, (in Japanese).
60 V. F. Petrenko and R. W. Whitworth, *Physics of Ice*, Oxford University Press, New York, 2nd edn, 2003.
61 W. G. Finnegan and R. L. Pitter, A postulate of electric multipoles in growing ice crystals: their role in the formation of ice crystal aggregates, *Atmos. Res.*, 1988, **22**, 235–250.
62 V. F. Petrenko, The surface of ice, *Cold Regions Research & Engineering Laboratory Special Report 94-22*, Thayer School of Engineering Dartmouth College, USA, 1994.
63 V. F. Petrenko and E. M. Schulson, The effect of static electric fields on protonic conductivity of ice single crystal, *Philos. Mag. B*, 1992, **66**, 341–353.
64 A. Sato and G. Wakahama, Measurement of the velocity of cracks propagation in ice, in *Physics and Chemistry of Ice*, ed. N. Maeno and T. Kondoh, Hokkaido University Press, Sapporo, 1992, pp. 476–480.
65 W. Gaskell and A. J. Illingworth, Charge transfer accompanying individual collisions between ice particles and its role in thunderstorm electrification, *Q. J. R. Meteorol. Soc.*, 1980, **106**, 841–854.
66 R. G. Pereyra and E. E. Avila, Charge transfer measurements during single ice crystal collisions with a target growing by riming, *J. Geophys. Res.*, 2002, **107**(D23), 4735–4744.
67 R. A. Lighezzolo, R. G. Pereyra and E. E. Avila, Measurements of electric charge separated during the formation of rime by the accretion of supercooled droplets, *Atmos. Chem. Phys.*, 2010, **10**, 1661–1669.
68 W. D. Keith and C. P. R. Saunders, Light emission from colliding ice particles, *Nature*, 1988, **336**, 362–364.
69 A. I. Grigor'ev and D. N. Doroshenko, Critical conditions for instability of an aqueous film on the surface of a stationary charged melting hailstone in an external electric field, *Fluid Dyn.*, 1987, **22**(1), 7–11.
70 R. W. Style and M. G. Worster, Frost flower formation on sea ice and lake ice, *Geophys. Res. Lett.*, 2009, **36**, L11501.
71 S. V. Nghiem, S. Martin, D. K. Perovich, R. Kwok, R. Drucker and A. J. Gow, A laboratory study of the effect of frost flowers on C band radar backscatter from sea ice, *J. Geophys. Res.*, 1997, **102**(C2), 3357–3370.
72 T. Gonda, Experimental studies of dendritic ice crystals growing from the vapor phase, in *Research of Pattern Formation*, ed. R. Takaki, KTK Scientific Publishers, Tokyo, 1994, pp. 122–130.
73 B. A. Tinsley, W. Liu, R. P. Rohrbaugh and M. W. Kirkland, South pole electric field responses to overhead ionospheric convection, *J. Geophys. Res.*, 1998, **103**(D20), 26137–26146.
74 E. Belova, S. Kirkwood and H. Tammet, The effect of magnetic substorms on near ground atmospheric current, *Ann. Geophys.*, 2001, **18**, 1623–1629.
75 S. Horton and B. Jamison, Spectral measurements of surface hoar crystals, *J. Glaciol.*, 2017, **63**(239), 477–486.
76 E. A. Bering III, A. A. Few and J. R. Benbrook, The global electric circuit, *Phys. Today*, 1998, **51**, 24–30.
77 C. G. Deshpande and A. K. Kamra, The atmospheric electric conductivity and aerosol measurements during fog over the Indian Ocean, *Atmos. Res.*, 2004, **70**, 77–87.
78 U. Nakaya, *Snow Crystals: Natural and Artificial*, Harvard University Press, Cambridge, 1954.
79 S. C. Colbeck, Theory of metamorphism of dry snow, *J. Geophys. Res.: Oceans*, 1983, **88**(9), 5475–5482.
80 E. Brun, P. David, M. Sudul and G. Brunot, A numerical model to simulate snow-cover stratigraphy for operational avalanche forecasting, *J. Glaciol.*, 1992, **38**, 13–22.
81 M. Sturm and C. S. Benson, Vapor transport, grain growth and depth-hoar development in the subarctic snow, *J. Glaciol.*, 1997, **43**, 42–59.
82 R. Granger, F. Flin, W. Ludwig, I. Hammad and C. Geindreau, Orientation selective grain sublimation–deposition in snow under temperature gradient metamorphism observed with diffraction contrast tomography, *Cryosphere*, 2021, **15**, 4381–4398.
83 B. Pinzer, M. Schneebeli and T. U. Kaempfer, Vapor flux and recrystallization during dry snow metamorphism under a steady temperature gradient as observed by time-lapse microtomography, *Cryosphere*, 2012, **6**, 1141–1155.

84 F. Flin and J.-B. Brzoska, The Temperature-Gradient Metamorphism of Snow: Vapour Diffusion Model and Application to Tomographic Images, *Ann. Glaciol.*, 2008, **49**, 17–21.
85 B. Pinzer and M. Schneebeli, Breeding snow: An instrumented sample holder for simultaneous tomographic and thermal studies, *J. Mech. Sci. Technol.*, 2009, **20**, 095705–095714.
86 B. Pinzer and M. Schneebeli, Snow metamorphism under alternating temperature gradients: Morphology and recrystallization in surface snow, *Geophys. Res. Lett.*, 2009, **36**, L23503.
87 A. K. Dunin, *Evaporation of Snow*, Sibirian Academy of Science of USSR, Novosibirsk, 1961, (in Russian).
88 D. A. Miller and E. E. Adams, A microstructural dry-snow metamorphism model for kinetic crystal growth, *J. Glaciol.*, 2009, **55**(194), 1003–1011.
89 N. A. Kazakov, Snow cover as an electrodynamic system, *Earth's Cryosphere*, 2017, **21**(2), 10–20.
90 R. Lord, On the Equilibrium of Liquid Conducting Masses Charged with Electricity, *Phil. Mag.*, 1882, **14**, 184–186.
91 C. D. Hendrics and J. M. Schneider, Stability of conducting droplet under the influence of surface tension and electrostatic forces, *Am. J. Phys.*, 1963, **31**, 450–453.
92 D. Duft, T. Achtzehn, R. Müller, B. A. Huber and T. Leisner, Coulomb fission: Rayleigh jets from levitated microdroplets, *Nature*, 2003, **421**(6919), 128.
93 N. N. Khusnatdinov and V. F. Petrenko, Experimental study of ice electrolysis under UV irradiation, *J. Phys. Chem. B*, 1997, **101**, 6208–6211.
94 E. Tkachenko, Electric phenomena as a possible driver of polar snow-air interactions: does this factor act synergistically with photoinduced effects?, *Int. J. Environ. Clim. Change*, 2019, **9**(9), 518–521.
95 K. S. Suslick, Chemical effects of Ultrasound, *Sci. Am.*, 1989, **260**(2), 80–86.
96 G. Santachiara, F. Prodi and F. Belosi, A Review of Termo- and Diffusio-Phoresis in the Atmospheric Aerosol Scavenging Process. Part 1: Drop Scavenging, *Atm. Climate Sciences*, 2012, **2**, 148–158.
97 T. E. Graedel and J. P. Franey, Field measurements of submicron aerosol washout by snow, *Geophys. Res. Lett.*, 1975, **2**, 325–328.
98 C. Magono, T. Endoh, T. Hariyama and S. Kuboda, A measurement of scavenging effect of falling snow crystals on the aerosol concentration, *J. Meteorol. Soc. Jpn.*, 1974, **52**, 407–416.
99 C. Magono, T. Endoh and M. Itasaka, Observation of aerosol particles attached to falling snow crystals, Part2, Utilizing an Electron microscope, *Journal of the Faculty of Science, Hokkaido University. Series 7, Geophysics*, 1976, **4**, 103–119.
100 M. Murakami, C. Hiramatsu and C. Magono, Observation of aerosol scavenging by falling snow crystals at two sites of different heights, *J. Meteorol. Soc. Jpn.*, 1981, **59**, 763–811.
101 S. M. Greenfield, Rain scavenging of radioactive particulate matter from the atmosphere, *J. Meteorol.*, 1957, **14**, 115–125.
102 T. Sparks and G. Chase, *Filters and Filtration Handbook. Section 3 – Air and Gas Filtration*, Elsevier Ltd, Oxford, UK, 6th edn, 2016, pp. 117–198.
103 R. Kuhn and S. Hofstetter-Kuhn, *Capillary Electrophoresis, Principle and Practice*, Springer-Verlag, Berlin, Heidelberg, 1993.
104 D. R. Baker, *Capillary Electrophoresis*, Wiley-Interscience, 1st edn, 1995.
105 L. Loeb, *Electrical Coronas: Their Basic Physical Mechanisms*, University of California Press, Berkeley, 1965, p. 694.
106 W. R. Simpson, R. von Glasow, K. Riedel, P. Anderson, P. Ariya, J. Bottenheim, J. Burrows, L. J. Carpenter, U. Frieß, M. E. Goodsite, D. Heard, M. Hutterli, H.-W. Jacobi, L. Kaleschke, B. Neff, J. Plane, U. Platt, A. Richter, H. Roscoe, R. Sander, P. Shepson, J. Sodeau, A. Steffen, T. Wagner and E. Wolff, Halogens and their role in polar boundary-layer ozone depletion, *Atmos. Chem. Phys.*, 2007, **7**, 4375–4418.
107 A. Steffen, T. Douglas, M. Amyot, P. Ariya, K. Aspmo, T. Berg, J. Bottenheim, S. Brooks, F. Cobbett, A. Dastoor, A. Dommergue, R. Ebinghaus, C. Ferrari, K. Gardfeldt, M. E. Goodsite, D. Lean, A. J. Poulain, C. Scherz, H. Skov, J. Sommar and C. Temme, A synthesis of atmospheric mercury depletion event chemistry in the atmosphere and snow, *Atmos. Chem. Phys.*, 2008, **8**, 1445–1482.
108 N. Benavent, A. S. Mahajan, Q. Li, C. A. Cuevas, J. Schmale, H. Angot, T. Jokinen, L. Quéléver, A.-M. Blechschmidt, B. Zilker, A. Richter, J. A. Serna, D. Garcia-Nieto, R. P. Fernandez, H. Skov, A. Dumitrascu, P. Simões Pereira, K. Abrahamsson, S. Bucci, M. Dütsch, A. Stohl, I. Beck, T. Laurila, B. Blomquist, D. Howard, S. Archer, L. Bariteau, D. Helmig, J. Hueber, H.-W. Jacobi, K. Posman, L. Dada, K. R. Dällenbach and A. Saiz-Lopez, Substantial contribution of iodine to Arctic ozone destruction, *Nat. Geosci.*, 2022, **15**, 770–773.
109 R. Vogt, P. J. Crutzen and R. Sander, A mechanism for halogen release from sea-salt aerosol in the remote marine boundary layer, *Nature*, 1996, **383**, 327–330.
110 H.-W. Jacobi, L. Kaleschke, A. Richter, A. Rozanov and J. P. Burrows, Observation of a fast ozone loss in the marginal ice zone of the Arctic Ocean, *J. Geophys. Res.*, 2006, **111**, D15309.
111 H.-W. Jacobi, D. Voisin, J.-L. Jaffrezo, J. Cozic and T. A. Douglas, Chemical composition of the snowpack during the OASIS spring campaign 2009 at Barrow, AK, *J. Geophys. Res.*, 2012, **117**, D00R13.
112 M. Nerentorp Mastromonaco, K. Gårdfeldt, B. Jourdain, K. Abrahamsson, A. Granfors, M. Ahnoff, A. Dommergue, G. Méjean and H.-W. Jacobi, Antarctic winter mercury and ozone depletion events over sea ice, *Atmos. Environ.*, 2016, **129**, 125–132.
113 W. R. Simpson, U. Frieß, J. L. Thomas, J. Lampel and U. Platt, Polar nighttime chemistry produces intense

reactive bromine events, *Geophys. Res. Lett.*, 2018, **45**, 9987–9994.

114 H.-W. Jacobi, S. Morin and J. W. Bottenheim, Observation of widespread depletion of ozone in the springtime boundary layer of the Central Arctic linked to mesoscale synoptic conditions, *J. Geophys. Res.*, 2010, **115**, D17302.

115 H. Angot, B. Blomquist, D. Howard, S. Archer, L. Bariteau, I. Beck, M. Boyer, M. Crotwell, D. Helmig, J. Hueber, H.-W. Jacobi, T. Jokinen, M. Kulmala, X. Lan, T. Laurila, M. Madronich, D. Neff, T. Petäjä, K. Posman, L. Quéléver, M. Shupe, I. Wimont and J. Schmale, Year-round trace gas measurements in the central Arctic during the MOSAiC expedition, *Sci. Data*, 2022, **9**, 723–742.

116 V. J. Schaefer, The generation of large numbers of ice crystals in an electric field, *J. Appl. Meteorol.*, 1968, **7**, 452–455.

117 V. J. Schaefer and R. J. Cheng, The production of ice crystals fragments by sublimation and electrification, *J. Rech. Atmos.*, 1971, **5**, 5–10.

118 F. K. Odencrantz, P. St. Amand, W. G. Finnegan and W. S. McEwan, Mechanism for multiplication of atmospheric ice crystals: apparent charge distribution on laboratory crystals, *Science*, 1968, **160**(3834), 1345–1346.

119 A. K. Kamra and D. V. Ahire, Electrical atomization of water dripping from melting ice pieces and its possible role in thunderstorms, *J. Clim. Appl. Meteorol.*, 1984, **23**, 845–847.

120 M. Yamashita and J. B. Fenn, Electrospray ion source, another variation of free jet theme, *J. Phys. Chem.*, 1984, **88**, 4451–4459.

121 S. Banerjee and S. Mazumdar, Electrospray Ionization Mass Spectrometry: A Technique to Access the Information beyond the Molecular Weight of the Analyte, *Int. J. Anal. Chem.*, 2012, **2012**(8), 282574–282614.

122 H. T. Nguyen, K. H. Kim, Z. H. Shon and S. Hong, A Review of Atmospheric Mercury in the Polar Environment, *Crit. Rev. Environ. Sci. Technol.*, 2009, **39**(7), 552–584.

123 X. P. Wang, C. F. Wang, T. T. Zhu, P. Gong, J. J. Fu and Z. Y. Cong, Persistent organic pollutants in the polar regions and the Tibetan Plateau: A review of current knowledge and future prospects, *Environ. Pollut.*, 2019, **248**, 191–208.

124 T. A. Douglas, M. Sturm, W. R. Simpson, S. Brooks, S. E. Lindberg and D. K. Perovich, Elevated mercury measured in snow and frost flowers near Arctic sea ice leads, *Geophys. Res. Lett.*, 2005, **32**, L04502.

125 L. S. Sherman, J. D. Blum, T. A. Douglas and A. Steffen, Frost flowers growing in the Arctic ocean-atmosphere–sea ice–snow interface: 2. Mercury exchange between the atmosphere, snow, and frost flowers, *J. Geophys. Res.*, 2012, **117**, D00R10.

126 T. A. Douglas, F. Domine, M. Barret, C. Anastasio, H. J. Beine, J. Bottenheim, A. Grannas, S. Houdier, S. Netcheva, G. Rowland, R. Staebler and A. Steffen, Frost flowers growing in the Arctic ocean-atmosphere–sea ice–snow interface: 1. Chemical composition, *J. Geophys. Res.*, 2012, **117**, D00R09.

127 D. L. Mitchell and D. Lamb, Influence of riming on the chemical composition of snow in winter orographic storms, *J. Geophys. Res.*, 1989, **94**, 14831–14840.

128 O. Poulida, M. Schwikowski, U. Baltensperger, J. Staehelin and H. W. Gäggeler, Scavenging of atmospheric constituents in mixed phase clouds at the High-Alpine site Jungfraujoch—Part II. Influence of riming on the scavenging of particulate and gaseous chemical species, *Atmos. Environ.*, 1998, **32**, 3985–4000.

129 J. R. Snider and J. Huang, Factors Influencing the Retention of Hydrogen Peroxide and Molecular Oxygen in Rime Ice, *J. Geophys. Res.*, 1998, **103**, 1405–1415.

130 Y. Long, N. Chaumerliac, L. Deguillaume, M. Leriche and F. Champeau, Effect of mixed-phase cloud on the chemical budget of trace gases: A modeling approach, *Atmos. Res.*, 2010, **97**, 540–554.

131 C. W. Moore, D. Obrist, A. Steffen, R. M. Staebler, T. A. Douglas, A. Richter and S. V. Nghiem, Convective forcing of mercury and ozone in the Arctic boundary layer induced by leads in sea ice, *Nature*, 2014, **506**, 81–84.

132 A. S. Mahajan, M. Shaw, H. Oetjen, K. E. Hornsby, L. J. Carpenter, L. Kaleschke, X. Tian-Kunze, J. D. Lee, S. J. Moller, P. Edwards, R. Commane, T. Ingham, D. E. Heard and M. C. Plane, Evidence of reactive iodine chemistry in the Arctic boundary layer, *J. Geophys. Res.*, 2010, **115**, D20303.

133 Atmospheric temperature, *Atmospheric Pressure, Wind, Atmospheric Humidity, Nebulosity, Precipitations, Meteors, Visibility*, ed. I. M. Dolgin and L. S. Petrov, Gidrometeoizdat, Leningrad, 1977, vol. 2, [in Russian].

134 J. H. Seinfeld, and S. N. Pandis, *Atmospheric Chemistry and Physics: From Air Pollution to Climate Change*, John Wiley & Sons, Hoboken, 2016.

135 R. L. Mauldin, D. J. Tanner and F. L. Eisele, Measurement of OH during PEM-Tropics A, *J. Geophys. Res.*, 1999, **104**(D5), 5817–5827.

136 A.-L. Sumner and P. B. Shepson, Snowpack production of formaldehyde and its effect on the Arctic troposphere, *Nature*, 1999, **398**, 230–233.

137 T. M. Dassau, A. L. Sumner, S. L. Koeniger, P. B. Shepson, J. Yang, R. E. Honrath, N. J. Cullen, K. Steffen, H.-W. Jacobi, M. Frey and R. C. Bales, Investigation of the role of the snowpack on atmospheric formaldehyde chemistry at Summit, Greenland, *J. Geophys. Res.*, 2002, **107**(D19), 4394.

138 A. E. Jones, R. Weller, E. W. Wolf and H.-W. Jacobi, Speciation and rate of photochemical NO and NO_2 production in Antarctic snow, *Geophys. Res. Lett.*, 2000, **27**, 345–348.

139 X. Zhou, H. Beine, R. E. Honrath, J. D. Fuentes, W. Simpson, P. B. Shepson and J. W. Bottenheim, Snowpack photochemical production of HONO: a major source of OH in the Arctic Boundary Layer in springtime, *Geophys. Res. Lett.*, 2001, **28**, 4087–4090.

140 H.-W. Jacobi, J. Kleffmann, G. Villena, P. Wiesen, M. King, J. France, C. Anastasio and R. Staebler, Role of nitrite for

the photochemical formation of radicals in the snow, *Environ. Sci. Technol.*, 2014, **48**, 165–172.

141 M. A. Hutterli, J. R. McConnell, R. W. Stewart, H.-W. Jacobi and R. C. Bales, Impact of temperature-driven cycling of hydrogen peroxide (H_2O_2) between air and snow on the planetary boundary layer, *J. Geophys. Res.: Atmos.*, 2001, **106**, 15395–15404.

142 A. M. Grannas, P. B. Shepson, C. Guimbaud, A. L. Sumner, M. Albert, W. Simpson, F. Domine, H. Boudries, J. Bottenheim, H. J. Beine, R. E. Honrath and X. Zhou, A study of photochemical and physical processes affecting carbonyl compounds in the Arctic atmospheric boundary layer, *Atmos. Environ.*, 2002, **36**, 2733–2742.

143 G. Chen, D. Davis, J. Crawford, L. M. Hutterli, L. G. Huey, D. Slusher, L. Mauldin, F. Eisele, D. Tanner, J. Dibb, M. Buhr, J. McConnell, B. Lefer, R. Shetter, D. Blake, C. H. Song, K. Lombardo and J. Arnoldy, A reassessment of HOx South Pole chemistry based on observations recorded during ISCAT 2000, *Atmos. Environ.*, 2004, **38**, 5451–5461.

144 J. Yang, R. E. Honrath, M. C. Peterson, J. E. Dibb, A. L. Sumner, P. B. Shepson, M. Frey, H.-W. Jacobi, A. Swanson and N. Blake, Impacts of snowpack emissions on deduced levels of OH and peroxy radicals at Summit, Greenland, *Atmos. Environ.*, 2002, **36**, 2523–2534.

145 H.-W. Jacobi, R. C. Bales, R. E. Honrath, M. C. Peterson, J. E. Dibb, A. L. Swanson and M. R. Albert, Reactive trace gases measured in the interstitial air of surface snow at Summit, Greenland, *Atmos. Environ.*, 2004, **38**, 1687–1697.

146 D. Helmig, B. Johnson, S. J. Oltmans, W. Neff, F. Eisele and D. Davis, Elevated ozone in the boundary layer at South Pole, *Atmos. Environ.*, 2008, **42**, 2788–2803.

147 J. France, H. Reay, M. King, D. Voisin, H.-W. Jacobi, F. Domine, H. Beine, C. Anastasio, A. MacArthur and J. Lee-Taylor, Hydroxyl radical and NOx production rates, black carbon concentrations and light-absorbing impurities in snow from field measurements of light penetration and nadir reflectivity of on-shore and off-shore coastal Alaskan snow, *J. Geophys. Res.*, 2012, **117**, D00R12.

148 D. Helmig, F. Bocquet, L. Cohen and S. J. Oltmans, Ozone uptake to the polar snowpack at Summit, Greenland, *Atmos. Environ.*, 2007, **41**(24), 5061.

149 A. Barbero, J. Savarino, R. Grilli, C. Blouzon, G. Picard, M. M. Frey, Y. Huang and N. Caillon, New estimation of the NOx snow-source on the Antarctic Plateau, *J. Geophys. Res.: Atmos.*, 2021, **126**, e2021JD035062.

150 A. Virkkula, A. Hirsikko, M. Vana, P. P. Aalto, R. Hillamo and M. Kulmala, Charged particles size formation events at the Finnish Antarctic research station Aboa, *Boreal Environ. Res.*, 2007, **12**, 397–408.

151 W. R. Simpson, S. S. Brown, A. Saiz-Lopez, J. A. Thornton and R. A. Glasow, Tropospheric Halogen Chemistry: Sources, Cycling, and Impacts, *Chem. Rev.*, 2015, **115**(10), 4035–4062.

152 K. L. Foster, R. A. Plastridge, J. W. Bottenheim, P. B. Shepson, B. J. Finlayson-Pitts and C. W. Spicer, The role of Br2 and BrCl in surface ozone destruction at polar sunrise, *Science*, 2001, **291**(5503), 471–474.

153 L. Bouvet, N. Calonne, F. Flin and C. Geindreau, Heterogeneous grain growth and vertical mass transfer within a snow layer under a temperature gradient, *The Cryosphere*, 2023, **17**, 3553–3573.

154 R. E. Gagnon, Generation of melt during crushing experiments on freshwater ice, *Cold Reg. Sci. Technol.*, 1994, **22**(4), 385–398.

155 H.-W. Jacobi, B. Kwakye-Awuah and O. Schrems, Photochemical decomposition of hydrogen peroxide (H_2O_2) and formaldehyde (HCHO) in artificial snow, *Ann. Glaciol.*, 2004, **39**, 29–33.

156 H.-W. Jacobi and B. Hilker, A mechanism for the photochemical transformation of nitrate in snow, *J.Photochem.Photobiol.*, 2007, **185**, 371–382.

157 H.-W. Jacobi, T. Annor and E. Quansah, Investigation of the photochemical decomposition of nitrate, hydrogen peroxide, and formaldehyde in artificial snow, *J. Photochem. Photobiol., A*, 2006, **179**, 330–338.

158 K. Yu. Tkachenko, O. A. Varzatskii and M. A. Lozovoy, Cold combustion as a new method of toxic waste destruction, *ScienceRise*, 2015, **5/2**(10), 106–110.

159 P. J. H. Williams, G. A. Boustead, D. E. Heard, P. W. Seakins, A. R. Rickard and V. Chechik, New Approach to the Detection of Short-Lived Radical Intermediates, *J. Am. Chem. Soc.*, 2022, **144**(37), 15969–15976.

160 V. N. Belevskii and S. I. Belopushkin, Mechanism of the conversions of intermediate particles in liquid-phase radiolysis of acetic and propionic acids, investigated by ESR, *High Energy Chem.*, 1991, **25**(5), 342–348.